Journal for ImmunoTherapy of Cancer

Exosomal circPOLQ promotes macrophage M2 polarization via activating IL-10/STAT3 axis in a colorectal cancer model

Zhenqiang Sun ,[1,2] Yanxin Xu,[1,2] Bo Shao,[1,3] Pengyuan Dang,[1] Shengyun Hu,[1] Haifeng Sun,[1] Chen Chen,[2] Chaoguan Wang,[4] Jinbo Liu,[1] Yang Liu,[4] Junhong Hu[1,3]

To cite: Sun Z, Xu Y, Shao B, *et al*. Exosomal circPOLQ promotes macrophage M2 polarization via activating IL-10/STAT3 axis in a colorectal cancer model. *Journal for ImmunoTherapy of Cancer* 2024;**12**:e008491. doi:10.1136/jitc-2023-008491

► Additional supplemental material is published online only. To view, please visit the journal online (https://doi.org/10.1136/jitc-2023-008491).

ZS, YX and BS contributed equally.

YX are joint first authors.

BS are joint first authors.

Accepted 06 May 2024

Check for updates

© Author(s) (or their employer(s)) 2024. Re-use permitted under CC BY-NC. No commercial re-use. See rights and permissions. Published by BMJ.

For numbered affiliations see end of article.

Correspondence to
Professor Zhenqiang Sun; fccsunzq@zzu.edu.cn

Jinbo Liu; fccliujb@zzu.edu.cn

Dr Yang Liu; zlyyliuyang1440@zzu.edu.cn

Junhong Hu; hujunhong@zzu.edu.cn

ABSTRACT

Background Accumulating evidence demonstrates that an increased tumor-associated macrophage abundance is often associated with poor prognosis in colorectal cancer (CRC). The mechanism underlying the effect of tumor-derived exosomes on M2 macrophage polarization remains elusive.

Results The novel circular RNA circPOLQ exhibited significantly higher expression in CRC tissues than in paired normal tissues. Higher circPOLQ expression was associated with poorer prognosis in patients with CRC. In vitro and in vivo experiments showed that tumor-derived exosomal circPOLQ did not directly regulate CRC cell development but promoted CRC metastatic nodule formation by enhancing M2 macrophage polarization. circPOLQ activated the interleukin-10/signal transducer and activator of transcription 3 axis by targeting miR-379–3 p to promote M2 macrophage polarization.

Conclusion circPOLQ can enter macrophages via CRC cell-derived exosomes and promote CRC metastatic nodule formation by enhancing M2 macrophage polarization. These findings reveal a tumor-derived exosome-mediated tumor–macrophage interaction potentially affecting CRC metastatic nodule formation.

WHAT IS ALREADY KNOWN ON THIS TOPIC

⇒ The propensity for distant metastasis in colorectal cancer (CRC) significantly contributes to the adverse prognosis and diminished long-term survival rates among patients with CRC. Emerging evidence underscores the pivotal role of exosomes within the tumor microenvironment (TME) in facilitating intercellular communication by transferring critical biomolecules such as RNAs and proteins. Tumor-associated macrophages (TAMs) are known to actively internalize these exosomes, thereby adopting an immunosuppressive stance that fosters tumor metastasis. However, the underlying mechanisms remain elusive. Therefore, identifying metastasis-associated driver genes and viable therapeutic interventions to inhibit tumor metastasis holds paramount importance for enhancing treatment outcomes and prognoses in patients with CRC.

WHAT THIS STUDY ADDS

⇒ This study demonstrates that circRNAPOLQ exhibits high expression levels in CRC tissues, correlating with adverse prognostic outcomes. Both in vivo and in vitro models corroborate that circRNAPOLQ is conveyed to macrophages via exosomes derived from CRC cells. On internalization by macrophages, exosomal circRNAPOLQ targets miR-379–3 p, leading to the activation of the interleukin-10/signal transducer and activator of transcription 3 axis, driving the polarization towards an M2 phenotype, and ultimately facilitating the metastasis of CRC.

HOW THIS STUDY MIGHT AFFECT RESEARCH, PRACTICE OR POLICY

⇒ We explore a novel mode of TME formation where exosome-mediated communication between CRC cells and TAMs promotes CRC metastatic nodule formation. Additionally, this study presents evidence that exosome-derived circRNAPOLQ serves as a novel potential prognostic and therapeutic marker for CRC metastatic nodule formation.

INTRODUCTION

Tumor metastasis is an important cause of cancer-related death. Approximately 15–25% of colorectal cancers (CRCs) exhibit metastasis at the initial diagnosis.[1] Therefore, exploring tumor metastasis-related driver genes, potential mechanisms, and effective therapeutic targets to block tumor metastasis is highly important for improving the treatment efficacy and prognosis of patients with tumor metastasis.

The tumor microenvironment (TME) plays a crucial role in tumor growth and metastasis.[2] Research has demonstrated that cells within the TME actively participate in facilitating tumor metastasis.[3 4] Tumor-associated macrophages (TAMs), the predominant immune cells within the TME, release a spectrum of cellular chemokines and cytokines to augment the proliferation, invasion, and metastasis of tumor cells.[5 6] TAMs are predominantly polarized toward the M2 phenotype

and exhibit immunosuppressive and tumor progression-promoting effects.[7–9] Hence, the potential strategies for antitumor immunotherapy involve targeting M2-like TAMs and depleting them within the TME or repolarizing M2-like TAMs toward the M1-like phenotype. This approach directly enhances their cytotoxicity and indirectly stimulates cytotoxic T cells to eradicate tumor cells.

Exosomes are membrane-bound extracellular vesicles that have a diameter ranging from 30 to 150 nm.[10] Exosomes contain various biomolecules, such as proteins, DNA, and RNA. When exosomes are released into the extracellular environment, they are taken up by recipient cells, allowing their contents to be transferred to recipient cells. This process facilitates intercellular communication.[11] Mounting evidence suggests that exosomes play a significant role in TME and tumor metastasis. This is achieved through the transfer of signal peptides, noncoding RNAs, or DNA to adjacent cells or tissues.[12–14] Circular RNAs (circRNAs) are RNA molecules that are covalently closed and exhibit a wide range of roles, remarkable stability, and evolutionary conservation.[15] CircRNAs possess a distinct covalently closed loop structure and exhibit a unique tertiary structure. They are predominantly localized in the cytoplasm and play multifaceted roles in various cellular processes.[16] Several studies have reported that circRNAs are involved in tumorigenesis and tumor progression.[17 18] Exosomal circRNAs are taken up by nearby or distant cells, thereby regulating the functions of the recipient cells.[19] However, the specific interactions and mechanisms linking circRNAs and TAMs are unknown. CircRNAs are anticipated to emerge as novel tumor markers and potential targets for therapeutic intervention. These findings hold promise for opening new avenues for tumor diagnosis and targeted therapy.

In this study, we identified a novel circRNA, circPOLQ, known as circRNA4234. We evaluated the expression of circPOLQ in CRC through a series of clinical sample analyses in vitro and in vivo. We assessed whether CRC cell-derived exosomes induce M2 polarization of macrophages through the secretion of circPOLQ and explored the role and underlying mechanisms of circPOLQ in TAMs. These findings will help to identify new prognostic markers and provide a theoretical basis for developing potential tumor-targeted drugs.

MATERIALS AND METHODS

Patient tissue specimens and follow-up

Six pairs of matched CRC tissues and matched adjacent normal tissues were obtained from surgically resected patients at the First Affiliated Hospital of Zhengzhou University. Our previous study confirmed the reliability of this cohort.[20] Human CRC and adjacent normal mucosa samples were collected from patients with CRC who underwent surgical procedures at the First Affiliated Hospital of Zhengzhou University between January 2017 and September 2021. 28 CRC tissues were surgically removed from the patients. These patients did not receive any anticancer therapy. The clinical data of these tissues are shown in online supplemental table S1.

Cell culture

The HCT116, LoVo, HT-29, SW620, FHC (normal human colon epithelium cell line), THP-1 (human monocytic cell line), and 293T (human embryonic kidney 293 cell line) cell lines were acquired from the Type Culture Collection, Chinese Academy of Sciences (Shanghai, China). The human CRC cell line SW480 was obtained from the Biotherapy Center of The First Affiliated Hospital of Zhengzhou University. HCT116, LoVo, HT29, SW480, SW620, FHC, and 293T cells were cultured in high-glucose DMEM (Gibco, USA) supplemented with 10% fetal bovine serum (Bio Industries, Cromwell, Connecticut, USA) at 37°C and 5% CO_2. THP-1 cells were cultured in RPMI-1640 (Gibco, USA) supplemented with 10% fetal bovine serum (Bio Industries, Cromwell, Connecticut, USA). To induce THP-1 to differentiate into macrophages, THP-1 cells (1×10^6) were treated with 100 ng/mL phorbol 12-myristate 13-acetate (PMA; Sigma, USA) for 48 hours.

Cell transfection

siRNAs targeting circPOLQ and interleukin 10 (IL-10), miR-379–3p mimics, and inhibitors were designed and synthesized by RiboBio (Guangzhou, China). circPOLQ overexpression plasmids were constructed using GV689 as the vector, and IL-10 overexpression plasmids were constructed using GV657 as the vector by GeneChem (Shanghai, China). The sequences of the siRNAs, mimics, and inhibitors used are listed in online supplemental table S2. siRNAs and miR-379–3p mimics and inhibitors were transiently transfected into cells using Lipofectamine 3000 (Invitrogen, Thermo Fisher Scientific, Carlsbad, California, USA) following the manufacturer's instructions. All the sequences used in this study are summarized in online supplemental tables S2–S5.

Construction of stable cell lines

The lentiviral circPOLQ overexpression plasmid, along with the pSPAX2 and pMD2G plasmids, was transfected into 293T cells for viral packaging by GeneChem (Shanghai, China). The concentrated virus was then subjected to lentiviral transduction of HCT116 cells using LipoFilter Reagent. The cells were cultured with puromycin (2 µg/mL) to establish stable cell lines.

Nuclear and cytoplasmic extraction

RNA was extracted from the nuclear and cytoplasmic fractions using the PARIS Kit (Invitrogen, Thermo Fisher Scientific, Carlsbad, California, USA) following the manufacturer's instructions. Then, the expression of circPOLQ was detected by realtime fluorescence quantitative polymerase chain reaction (RT-qPCR).

Isolation and analysis of exosomes

For exosome isolation, supernatants collected from 3-day cell cultures were first centrifuged at 500×g for 10 min

to remove any cellular contamination. Subsequently, the supernatant was centrifuged at 12,000×g for 20 min to eliminate any potential apoptotic bodies or large cell debris. Furthermore, the exosomes were enriched by centrifugation at 100,000×g for 70 min at 4°C, and the resulting pellet was then washed with 200 µL of phosphate-buffered saline (PBS). The number and morphology (cup-shaped) of the exosomes were examined using a NanoSight NS300 microscope (Malvern Instruments, UK) and a Philips CM120 BioTwin transmission electron microscope (FEI Company, USA).

RNA isolation, reverse transcription, and qPCR

Total RNA was extracted using RNAiso Plus reagent (Takara, Dalian, China). Then, the RNA was reverse transcribed into complementary DNA (cDNA) using the PrimeScript RT Master Mix Kit (Takara, Dalian, China), followed by RT-qPCR using Hieff qPCR SYBR Green Master Mix (Low Rox Plus) (Yeasen, Shanghai, China) according to the manufacturer's instructions. Online supplemental table S3 lists all the primers used. All the data were normalized to the GAPDH data after analysis.

Identification of circRNAs

CRC cells were cultured with 100 ng/mL actinomycin D (Merck, Darmstadt, Germany) for 0 hour, 4 hours, 8 hours, 12 hours, and 16 hours. Total RNA was extracted, and the expression of circPOLQ and POLQ was detected via qPCR. In addition, convergent and divergent primers were designed, synthesized, and verified on the cDNA and genomic DNA (gDNA) of HCT116 and SW620 cells, respectively. Online supplemental table S4 lists the divergent and convergent primers used.

Western blot analysis

Total protein was extracted using the radio immunoprecipitation assay (RIPA) buffer (Solarbio, Beijing, China) supplemented with phenylmethanesulfonyl fluoride (PMSF) and a phosphatase inhibitor (CWBIO, China), and protein was quantified using a BCA kit (Bicinchoninic Acid Assay Kit, Beyotime, China). The proteins were then separated by 8% or 10% SDS-PAGE and transferred to polyvinylidene fluoride (PVDF) membranes (Millipore, Massachusetts, USA). The PVDF membranes were blocked with tris buffered saline with tween-20 (TBST) containing 5% (bovine serum albumin) BSA (Solarbio, Beijing, China). The membranes were incubated overnight at 4°C with the following primary antibodies: anti-CD206 (EPR22489-7), anti-TSG101 (Ab125011), anti-CD9 (Ab236630), and anti-STAT3 (Ab68153) from Abcam (Massachusetts, USA), anti-phospho-STAT3 (Tyr705) (#AF3293) from Affinity (Jiangsu, China), anti-ZO-1 (No. 21773–1-AP), anti-ZEB1 (No. 21544–1-AP), anti-α-SMA (No. 80008–1-RR), and anti-E-cadherin (No. 20874–1-AP) from Proteintech (Wuhan, China). The membrane was incubated with the secondary antibody for 1 hour at room temperature. The bands were visualized using a Chemiluminescence Kit (Millipore, USA).

RNA in situ hybridization and fluorescence in situ hybridization

For in situ hybridization (ISH), tissue sections were deparaffinized, incubated with a prehybridization solution, and subsequently hybridized with the circPOLQ probe (Servicebio, Wuhan, China). Then, the tissue sections were visualized using 3,3'-diaminobenzidine (DAB). The H-score was determined by Wuhan Sevier Biotechnology for fluorescence in situ hybridization (FISH). CRC cells were fixed with 4% paraformaldehyde in PBS for 20 min at room temperature. Hybridization of the Cy3-circPOLQ probe (GenePharma, Shanghai, China) was performed using a FISH kit (RiboBio, Guangzhou, China) following the manufacturer's instructions. Images were acquired using a confocal laser scanning microscope (Zeiss, Jena, Germany). The probe sequences can be found in online supplemental table S5.

Immunohistochemistry

Paraffin-embedded specimens were sectioned at a thickness of 3 µm. The sections were dewaxed and deparaffined in xylene and rehydrated in a graded alcohol series. The antigen retrieval process was performed by incubating the sections in Tris-EDTA buffer for 30 min. Subsequently, the primary antibodies against CD206 (No. 60143–1-Ig, Proteintech, Wuhan, China), CD163 (No. 16646–1-AP, Proteintech, Wuhan, China), N-cadherin (No. 22018–1-AP, Proteintech, Wuhan, China), VIM (No. 10366–1-AP, Proteintech, Wuhan, China) and their respective secondary antibodies were used for staining. Counterstaining with hematoxylin was then performed, followed by dehydration and mounting. Images of each section were taken in three randomly selected three fields of view under a microscope. The image analysis software ImageJ and Image-Pro Plus were used for data analysis.

Fluorescent labeling and tracking of CRC exosomes into macrophages

Exosomes derived from the CRC cell lines HCT116 and SW620 were labeled with PKH67 (green PKH membrane mini labeling kit, Sigma, Germany). Then, the above-pretreated exosomes were coincubated with THP-1-derived macrophages in 24-well plates for 0 hour, 6 hours, or 12 hours. The internalization of exosomes was examined using an LSM780 confocal laser scanning microscope (Zeiss, Germany). The nuclei of THP-1-derived macrophages were stained with 4',6-diamidino-2-phenylindole (Yeasen, Shanghai, China), and the cytoskeleton was stained with a microfilament protein (F-actin; GenePharma, Shanghai, China).

RNA pull-down assay

The biotinylated miR-379–3 p probe and negative control probe were designed and synthesized by GenePharma (Shanghai, China). The probe (30 µg) and 40 µL of streptomycin-coated magnetic beads were incubated for 30 min at room temperature. Cells were lysed in RNA binding protein immunoprecipitation assay (RIP) buffer

supplemented with a mixture of ribonuclease inhibitors and protease inhibitors. Cell extracts and probe bead complexes were mixed and incubated for 4 hours at 4°C with rotation. After rinsing with RIP wash buffer, the plates were digested with proteinase K digestion buffer at 900 rpm for 30 min at 55°C. The final RNA was extracted and reverse transcribed with an RNA Clean & Concentrator–25 kit (Zymo Research, USA) and a RevertAid First Strand cDNA Synthesis Kit (Thermo Fisher Scientific, Carlsbad, California, USA) for reverse transcription. The abundance of circPOLQ and IL-10 was then analyzed via qPCR.

Luciferase reporter assay

To generate the luciferase construct, the circPOLQ and IL-10 genes containing the miR-379–3 p binding site were synthesized by GeneChem (China) and inserted into the GV272 vector. Next, PMA-treated THP-1 cells were treated with IL-10-3′-UTR-Luc firefly luciferase constructs (wild-type or mutant) using Lipofectamine 3000 reagent (Invitrogen, USA). The Luc firefly luciferase construct (wild-type or mutant) was co-transfected with an miR-379–3 p mimic. Finally, 48 hours after transfection, the cell lysates were collected, and the firefly/Renilla luminescence was quantified using a Veritas 96-well microplate luminometer (Promega, USA) following the procedure of the Dual-Luciferase Reporter Assay Kit procedure (Biyuntian, China). Neutase activity was assessed using a substrate dispenser from Promega (USA). Renilla luciferase activity was normalized to firefly luciferase activity.

Transwell assay

Validation of CRC cell migration and invasion using the Transwell assay. This experiment was performed using a Transwell 24-well chamber (Corning, USA) with an 8.0 µm pore size polycarbonate membrane. For the invasion assay, additional diluted Matrigel (Corning, USA) was added to the chamber of a 24-well Transwell plate. To summarize, 5×10^4 tumor cells suspended in 200 µL of serum-free medium were seeded in the upper chamber, while the lower chamber contained 600 µL of medium supplemented with 10% fetal bovine serum (FBS). After 48 hours of incubation at 37°C in a 5% CO_2 humidified atmosphere, the migrated or invaded cells in the bottom chamber were fixed with paraformaldehyde and stained with 0.1% crystal violet. Three fields of view were randomly selected for imaging under a microscope. Photoshop software was used for statistical analysis.

Flow cytometry analysis

The cells were digested and collected by pancreatic enzymes, washed with PBS, and stained on ice with Fixable Viability Stain 700 (564997, BD Pharmingen, USA) for 10 min, followed by centrifugation in PBS to terminate the staining and incubation in a room temperature Fc blocker (422301, BioLegend, USA) for 15 min. The surface marker antibodies CD11b (301404, BioLegend, USA), CD206 (321105, BioLegend, USA), CD301 (354705, BioLegend, USA), and CD200R (329311, BioLegend, USA) were stained on ice in the dark for 30 min. Afterward, the cells were washed with PBS. The samples were analyzed using a DxFLEX flow cytometer (Beckman Coulter, USA) and the data were analyzed using FlowJo V.10.8.1.

Animal models

To investigate the functional role of circPOLQ in CRC-derived exosomes in vivo, we developed models of liver and lung metastasis using 6-week-old, pathogen-free, female NOD/SCID gamma (NSG) mice with severe immunodeficiency. These mice, procured from the Vital River Laboratory in Beijing, were maintained in a specific pathogen-free environment within our animal research facility. We isolated exosomes secreted by HCT116 cells that stably overexpressed circPOLQ and incubated them with mature macrophages induced by PMA for 48 hours. The SW480 cell line, stably transfected with luciferase, was subsequently co-cultured with the supernatant of the above macrophages. We harvested these SW480 cells by injecting 2×10^6 cells into the tail vein (100 µL) or the spleen (50 µL) of the mice. The survival duration of the mice was meticulously monitored. After 30 days, the mice were anesthetized and subjected to imaging using the IVIS Illumina system (Caliper Life Sciences, USA). Subsequently, the mice were euthanized, and nodules from the lungs and liver were extracted for paraffin embedding, H&E staining, and immunohistochemical analysis.

An orthotopic CRC model was used.[21–23] In brief, HCT116 cells stably overexpressing circPOLQ (1×10^6) and THP-1-derived macrophages were first mixed in equal amounts.[24] After NSG mice were anesthetized, a 1.5 cm incision was made around the midline of the abdomen, and the cecum was exteriorized and kept moist with PBS. The mixed cells (50 µL) were injected into the cecal wall using a 32-G needle, and the injection site was covered with a cotton swab for 3 min to prevent cell leakage. The cecum was returned to the abdominal cavity, and the abdominal wall and skin were carefully sutured with attention to aseptic disinfection. Mice were regularly monitored for orthotopic tumor formation and distant metastasis using the IVIS Illumina system. Six weeks later, mice were euthanized, and in situ tumors located at the cecum, liver, and lung were collected for pathological analysis.

Statistical analysis

All the data were analyzed using Prism V.10.0 (GraphPad, San Diego, California, USA) and are presented as the mean±SEM. X^2 tests were conducted using SPSS Statistics V.21 (IBM, Chicago, Illinois, USA). Student's t-test was used to evaluate significant differences between two independent groups. Pearson's correlation coefficient (r) and two-tailed p values were used for correlation analysis. Survival curves were assessed using the log-rank (Mantel-Cox) test. A p value<0.05 was considered to indicate statistical significance. All experiments were

replicated at least three times. All the authors had access to the study data and had reviewed and approved the final manuscript.

RESULTS

Elevated circPOLQ expression is positively associated with poor prognosis in patients with metastatic CRC

To identify the potential circRNAs associated with CRC metastasis, we initially conducted high-throughput sequencing on six sets of CRC tissues and their corresponding paracancerous normal tissues. Subsequently, we acquired the expression profiles of the dysregulated circRNAs. This expression profile was also applied in our previous study. TAMs are the most prevalent immune cells in the TME. Therefore, as an essential component, TAMs have been reported to strongly affect tumor progression. First, we identified immune-related circRNAs by correlation analysis and generated a heatmap. circPOLQ was among the top ranked candidates and was significantly upregulated in CRC tissues (figure 1A–C). circRNAPOLQ is derived from chromosome 3:121203887–121217517 and consists of five adjacent exons in the POLQ gene (online supplemental figure 1A). To validate the circular structure of circPOLQ, we designed convergent and divergent primers targeting circPOLQ and found that it could be amplified from cDNA but not from gDNA (figure 1D and online supplemental table S4). Additionally, actinomycin D treatment of HCT116 and SW620 cells less potently reduced the half-life of circPOLQ than did treatment with linear POLQ (figure 1E and online supplemental figure 1B). Taken together, these findings suggest that circPOLQ has a stable circRNA ring structure. Furthermore, we discovered by RNA nuclear/cytoplasmic fractionation and FISH revealed that circPOLQ was localized mainly in the cytoplasm in HCT116 and SW620 cells, with a low proportion of circPOLQ localized in the nucleus (figure 1F,G and online supplemental figure 1C).

To further explore the circPOLQ expression pattern in CRC, we conducted ISH analysis on a total of 28 pairs of fresh CRC tumors and their corresponding adjacent normal mucosal tissues. The expression of circPOLQ was greater in CRC tissues than in normal tissues and in metastatic tissues than in non-metastatic tissues, as determined by the H-score determined by QuantCenter software. The ISH images showed a greater proportion of circPOLQ-positive CRC tissues than in normal tissues (figure 1H,I). These findings indicate that CRC progression and distant metastasis are highly linked to excessively high circPOLQ expression. Survival analysis revealed that patients with elevated circPOLQ expression had a significantly lower overall survival rate than did those with lower circPOLQ expression (figure 1J). Collectively, these findings suggest that circPOLQ significantly contributes to tumor progression and has a notable impact on the prognosis of patients with CRC.

circPOLQ promotes M2 macrophage polarization

First, the expression of circPOLQ was shown to be considerably downregulated in siRNA-transfected CRC cells (figure 2A). Interestingly, CCK-8 assays revealed that reducing the expression of circPOLQ did not affect proliferation. Transwell assays revealed that circPOLQ expression affected invasion in both tumor cell lines, although to a non-significant extent (figure 2B–D). However, our previous findings strongly indicate a significant association between circPOLQ expression and both the development and prognosis of CRC. Therefore, circPOLQ may indirectly regulate the malignant progression of tumor cells. TAMs have been extensively investigated due to their involvement in various key aspects of tumor biology, including tumor initiation, angiogenesis, metastasis, drug resistance, and modulation of the antitumor immune response.[25] CircRNAs influence TAMs to secrete growth factors, cytokines and chemokines and interact with tumor cells or other stromal cells.[26] We thus postulated that circPOLQ may affect CRC development by modulating TAMs.

To further validate our hypothesis, we first discovered that circPOLQ expression exhibited positive correlations with the expression of M2 macrophage markers and negative correlations with the expression of M1-type macrophage markers in the abovementioned sequencing data (figure 2E and online supplemental figure 2A). Hence, we assessed the expression of the M2 macrophage polarization marker CD163 in a set of 20 paired CRC tissues (figure 2F). The proportion of CD163-positive cells in CRC tissues was significantly greater than that in normal mucosal tissues (figure 2G). Moreover, in the same cohort, circPOLQ positivity was significantly correlated with CD163 positivity. Thus, we hypothesized that circPOLQ affects M2 macrophage polarization.

Subsequently, we successfully induced THP-1 cells to differentiate into macrophages. The morphology of the THP-1 cells was altered considerably after induction with PMA, during which the cells transitioned from an initial suspended state to an adherent state (online supplemental figure 2B). Consistent with these findings, qPCR revealed that the expression of the macrophage markers CD14 and CD11b was dramatically increased (online supplemental figure 2B). We then co-cultured macrophages with the supernatant from the tumor cell cultures. The group of macrophages co-cultured with tumor cells had significantly greater expression of M2 polarization markers than the group of macrophages not co-cultured with tumor cells. In contrast to that in the control group, the expression of M2 macrophage markers was considerably reduced in macrophages co-cultured with tumor cells with circPOLQ knockdown (figure 2H–K and online supplemental figure 2C–E). The abovementioned findings demonstrated that co-culturing of macrophages with supernatants of circPOLQ-expressing tumor cells increases M2 macrophage polarization.

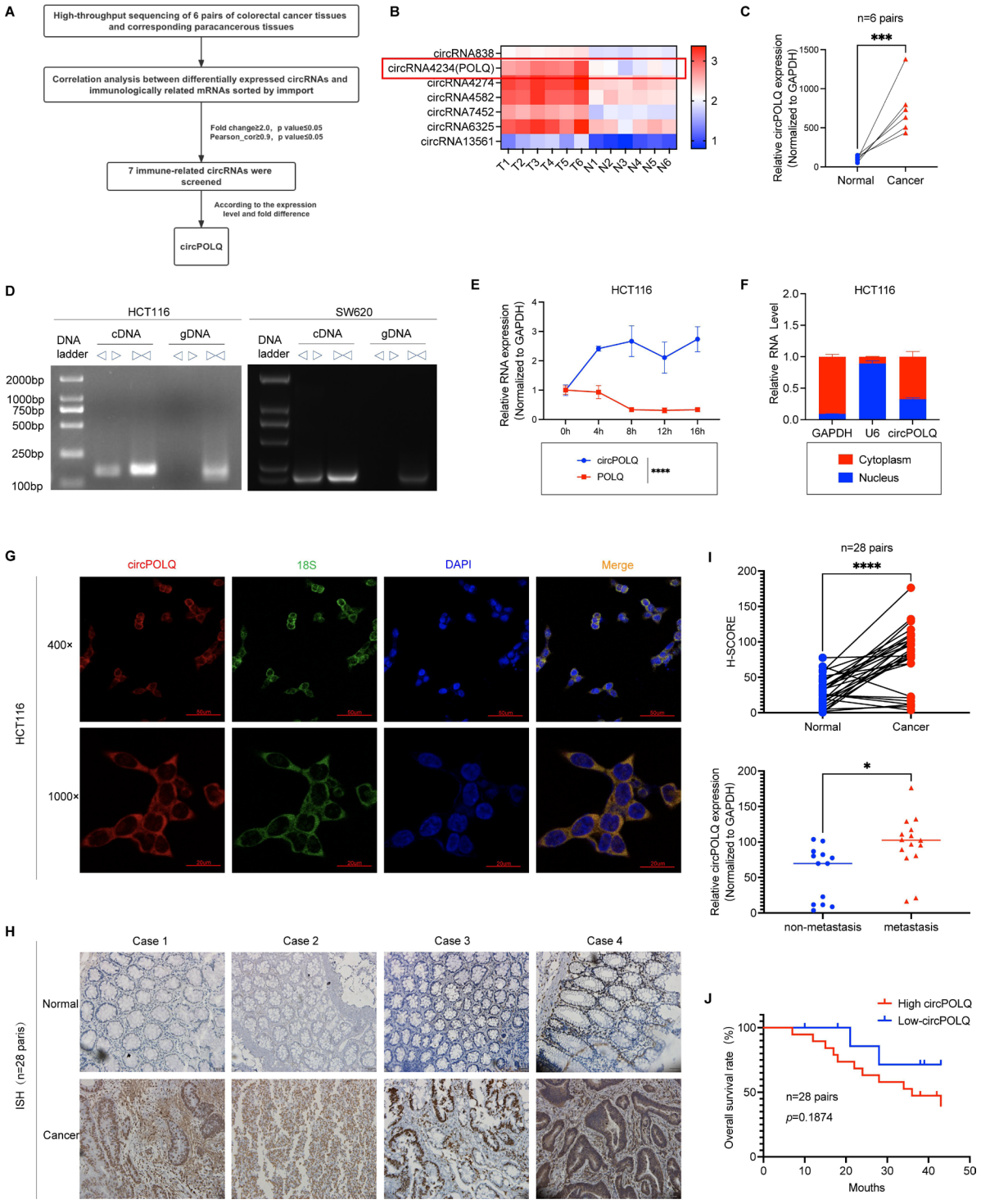

Figure 1 High expression of circPOLQ is positively related to poor prognosis of patients with CRC. (A) Flow chart for screening circRNAs in six pairs of CRC tissues. (B) Heatmap of deregulated circRNAs associated with immune mRNAs. (C) Expression of circPOLQ in the sequencing data of six pairs of CRC tissues and corresponding normal tissues. (D) Agarose gel analysis of PCR products using circPOLQ divergent primer and convergent primer. (E) qPCR analysis of circPOLQ and POLQ expression after culturing HCT116 cells with actinomycin D at 0 hour, 4 hours, 8 hours, 12 hours, and 16 hours. (F) Nuclear and cytoplasmic fractionation analysis assessed circPOLQ expression in HCT116 cytoplasmic fractionation. U6 and GAPDH were used as internal references. (G) Fluorescence in situ hybridization identified the location of circPOLQ in HCT116. (H) ISH images of circPOLQ in 28 pairs of CRC tissues and paired normal tissues. (I) H-scores of circPOLQ in 28 pairs of CRC tissues compared with corresponding normal tissues and H-scores of circPOLQ in CRC metastatic tissues compared with non-metastatic tissues (metastatic tissues number: 13; non-metastatic tissues number: 15). (J) Overall survival analysis of circPOLQ in 28 pairs of patients with CRC. Statistical significance was calculated by Student's t-test. Data in the text were expressed as mean±SD, *p<0.05, ***p<0.001, ****p<0.0001. cDNA, complementary DNA; circRNA, circular RNA; CRC, colorectal cancer; DAPI, 4',6-diamidino-2-phenylindole; gDNA, genomic DNA; ISH, in situ hybridization; mRNA, messenger RNA.

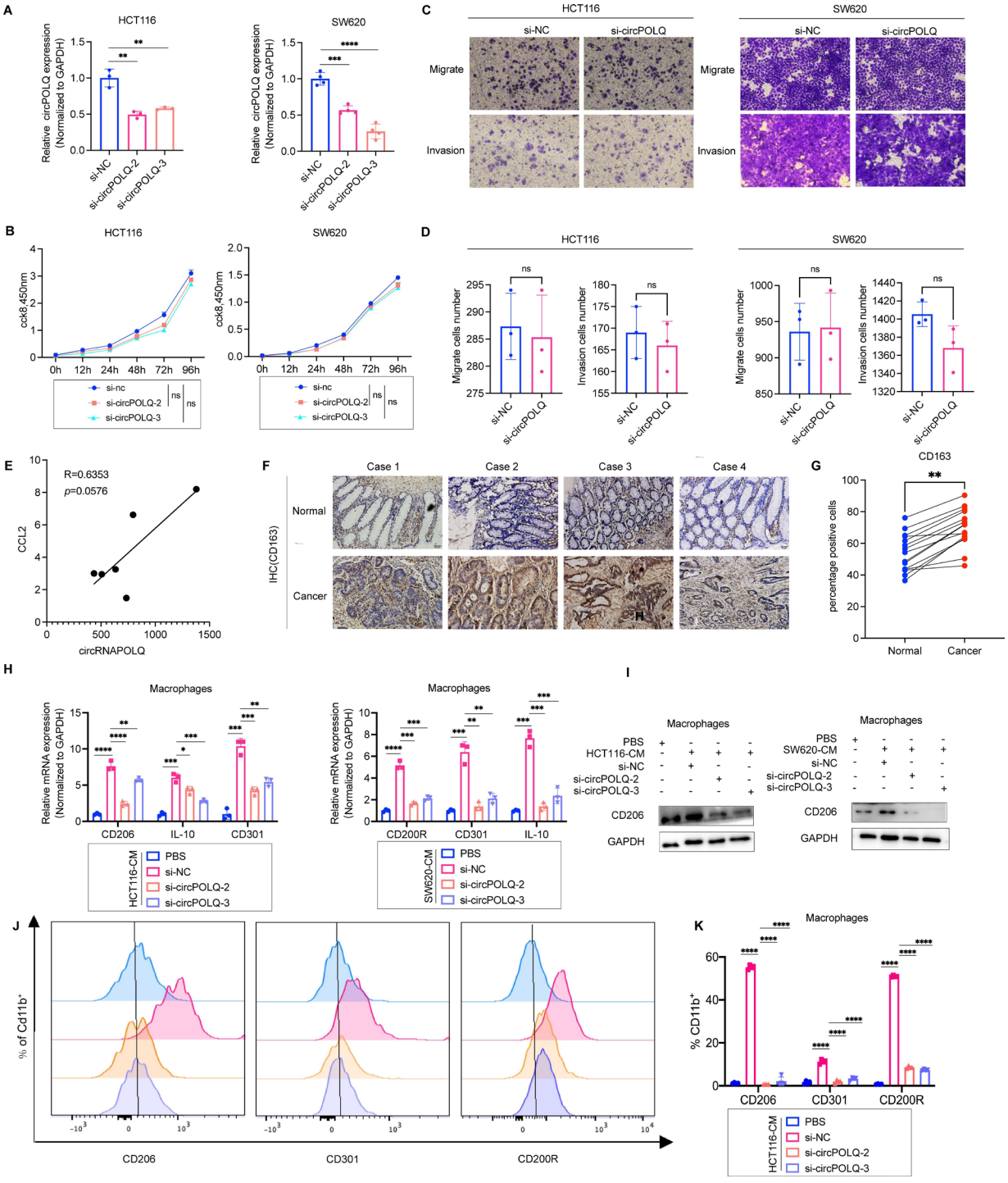

Figure 2 circPOLQ promotes macrophage M2 polarization. (A) qPCR analysis of si-circPOLQ efficiency in HCT116 and SW620 transfected with circPOLQ siRNA. (B) HCT116 and SW620 transfected with circPOLQ siRNA were used to evaluate tumor proliferation by CCK-8 assay. (C, D) Transwell assays of HCT116 cells and SW620 cells transfected with circPOLQ siRNA were used to assess migration and invasion. The number of migration and invasion was counted in HCT116 cells and SW620 cells. (E) Correlation analysis between circPOLQ and macrophage M2 polarization marker CCL2 in six pairs of CRC tissues and corresponding control tissues. (F) Representative IHC images from 4 of 20 analyzed tissue samples are shown, depicting positive staining for the pan-macrophage marker CD163 in CRC tissues. (G) The proportion of positive cells for macrophage pan-specific macrophage marker CD163 in CRC tissues detected by IHC. (H) qPCR analysis of expression of M2 polarization markers in PMA-pretreated THP-1 cells co-cultured with HCT116 and SW620. (I) Western blot analysis of expression of CD206 in PMA-pretreated THP-1 cells co-cultured with HCT116 cells and SW620 cells. (J, K) Flow cytometry analysis of expression and proportion of M2 polarization markers in PMA-pretreated THP-1 cells co-cultured with HCT116 cells. Statistical significance was calculated by the Student's t-test. Data in the text were expressed as mean±SD, *p<0.05, **p<0.01, ***p<0.001, ****p<0.0001. CRC, colorectal cancer; IHC, immunohistochemistry; mRNA, messenger RNA; PBS, phosphate-buffered saline; PMA, phorbol 12-myristate 13-acetate; qPCR, quantitative PCR.

Highly expressed CRC cell-derived exosomal circPOLQ enters macrophages

On the basis of our previous studies, we found that exosomes play a significant role in facilitating cell-to-cell communication. This finding suggested that circPOLQ present in tumor cells could enter macrophages through exosomes, thereby regulating the mechanism of macrophage polarization.[27] To confirm our hypothesis, we collected the culture supernatants of HCT116 and SW620 tumor cells. First, we used particle size analysis to measure the diameter of the isolated exosomes in our samples, and we found that the diameter ranged from 30 to 150 nm (figure 3A). In addition, we performed electron microscopy analysis of the extracted exosome samples, which also revealed a very typical exosome structure (figure 3B). We detected the presence of the exosome-specific proteins TSG101 and CD9 by western blotting (figure 3C), thus demonstrating the reliability of our isolated exosomes. Subsequently, we investigated the internalization of exosomes by macrophages. When macrophages were

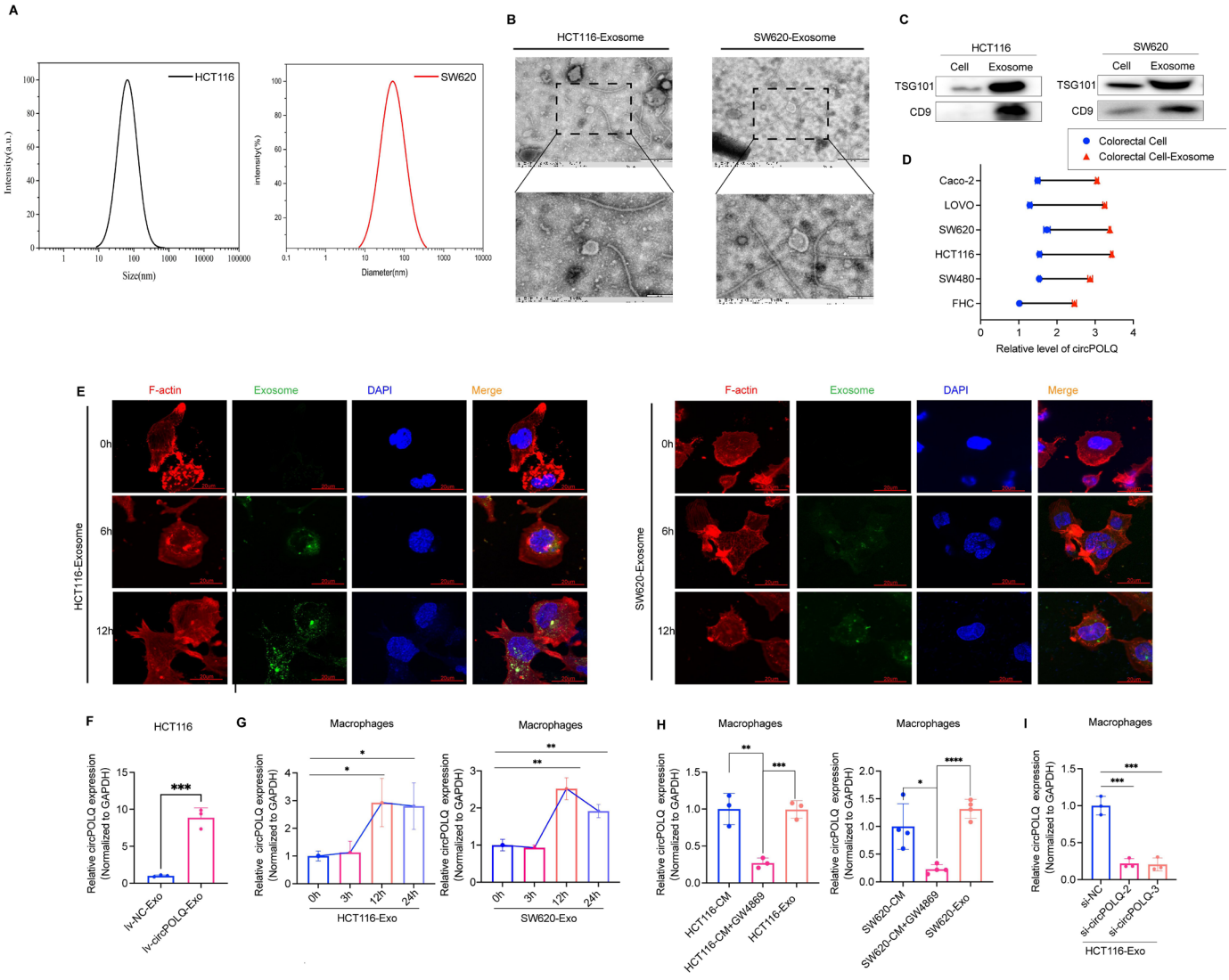

Figure 3 circPOLQ is encapsulated in CRC cell-derived exosomes and enters macrophages via exosomes. (A) Phenotypic analysis of exosomes derived from HCT116 and SW620 cells using NanoSight nanoparticle tracking. (B) Phenotypic analysis of exosomes derived from HCT116 and SW620 cells using electron microscopy. (C) Western blot analysis was performed to detect typical exosomal biomarkers (TSG101, CD9) in exosomes from HCT116, and SW620 cell lines. (D) Expression of circPOLQ in different CRC cell lines and FHC and their exosomes. (E) Immunofluorescence images showing internalization of PKH67-labeled HCT116 or SW620 cell-derived exosomes (green) in PMA-treated THP-1 cells. (F) The expression of circPOLQ in exosomes derived from HCT116 cells overexpressing circPOLQ was detected by qPCR. (G) The expression of circPOLQ was analyzed by qPCR after incubation of macrophages with HCT116, SW620 cell-derived exosomes for 0 hour, 3 hours, 12 hours, and 24 hours. (H) qPCR analysis of circPOLQ expression in conditioned medium-treated macrophages from HCT116, SW620 cells depleted of exosomes by GW4869. (I) The expression of circPOLQ in macrophages incubated with exosomes from tumor cells with knockdown of circPOLQ was detected by qPCR. Statistical significance was calculated by the Student's t-test. Data in the text were expressed as mean±SD, *p<0.05, **p<0.01, ***p<0.001, ****p<0.0001. CRC, colorectal cancer; DAPI, 4',6-diamidino-2-phenylindole; PMA, phorbol 12-myristate 13-acetate; qPCR, quantitative PCR.

coincubated with CRC cell-derived exosomes (labeled in green with PKH67), it was observed that the exosomes were successfully internalized by macrophages (labeled in red with F-actin) (figure 3E).

To further investigate whether circPOLQ enters macrophages via tumor cell-derived exosomes, we used qPCR to detect the expression of circPOLQ in various CRC cell lines, the normal colonic epithelial cell line FHC, and exosomes secreted from these cells. The expression of circPOLQ in CRC cell lines, particularly HCT116 and SW620 cells, as well as in their respective exosomes, was notably greater than that in FHC cells and their corresponding exosomes (figure 3D). Then, we generated an HCT116 cell line with stable circPOLQ overexpression and a control cell line and isolated exosomes from the culture supernatants of these two cell lines. Similar to the above findings, circPOLQ expression was dramatically elevated in exosomes secreted by the overexpression cell line (figure 3F and online supplemental figure 3A). The above assays demonstrated that circPOLQ is derived mainly from the exosomes released from CRC cells.

In addition, after incubating macrophages with 100 µg of exosomes, the expression of circPOLQ within the macrophages increased with increasing incubation time (figure 3G). GW4869 prevents exosome secretion from CRC cells. We observed significant downregulation of circPOLQ in macrophages incubated with supernatants from GW4869-treated tumor cells, and this downregulation was reversed by the addition of CRC cell-derived exosomes (figure 3H). Accordingly, we harvested culture supernatants from tumor cells transfected with massive quantities of si-circPOLQ and added the isolated exosomes to macrophages. Consistent with the prior results, circPOLQ expression was considerably lower in the experimental group than in the control group (figure 3I and online supplemental figure 3B). In addition, we replicated the aforementioned experiments in HCT116 cells stably overexpressing circPOLQ and in control cells, along with their corresponding exosomes (online supplemental figure 3C–G). Intriguingly, we observed that exosomes derived from the HCT116 cell lines with stable overexpression of circPOLQ appeared to be more abundant and were taken up by macrophages in greater quantities. These findings suggest the potential role of circRNAs in promoting exosome production and uptake by recipient cells, a process that warrants further mechanistic investigation to fully elucidate.

Taken together, these results indicate that circPOLQ is stably expressed in tumor cell-derived exosomes and enters macrophages via exosomes.

Exosomal circPOLQ induces M2 macrophage polarization, thereby promoting tumor cell migration and invasion

To further investigate the impact of circPOLQ on M2 macrophage polarization following transfer into macrophages via exosomes derived from CRC cells, we cultured macrophages in combination with exosomes obtained from tumor cells for 48 hours. By qPCR and western blotting, we found a significant increase in the expression of M2 macrophage polarization markers (online supplemental figure 4A,B). These results further support the hypothesis that circPOLQ may promote M2 macrophage polarization via exosomes. Moreover, we incubated M0 macrophages isolated from the si-NC and si-circPOLQ groups for 48 hours. By qPCR and western blotting, we found that the expression of M2 polarization markers was significantly greater in macrophages cultured with exosomes from the si-NC group than in those from the PBS group but was lower in macrophages incubated with exosomes from the si-circPOLQ group than in those from the si-NC group (figure 4A,B). Moreover, the expression of M1 polarization markers in macrophages cultured with exosomes from the si-NC group did not increase compared with that in the PBS group, and there was no difference in the expression of macrophages cultured with exosomes from the si-circPOLQ group compared with that in the si-NC group (figure 4A,B). In summary, these findings provide compelling evidence that exosomal circPOLQ derived from CRC cell lines effectively induces M2 polarization of macrophages.

Several studies have reported that tumor-derived exosome-induced M2 polarization of macrophages promotes CRC metastasis.[28 29] Therefore, we investigated whether M2 macrophages polarized by exosomal circPOLQ also supported the capacity of CRC cells to invade and metastasize. We cultured the CRC cell line SW480, which has low metastatic potential, for 24–48 hours in culture supernatant from THP-1-derived macrophages pretreated with exosomes from circPOLQ-knockdown HCT116 and SW620 cells.[30–33] Transwell assays revealed that, when co-cultured with culture supernatant obtained from THP-1-derived macrophages pretreated with exosomes derived from tumor cells, SW480 cells had significantly greater migratory and invasive capabilities than did SW480 cells in the control group treated with normal supernatant (PBS-treated). In addition, compared with those in the NC group, the migration and invasion abilities of SW480 cells co-cultured with culture supernatants from THP-1-derived macrophages pretreated with exosomes from the si-circPOLQ group were significantly lower (figure 4C–F). Furthermore, the expression of key epithelial-mesenchymal transition (EMT) proteins was altered. We found a significant increase in the expression of the EMT-related molecules zinc finger E-box binding homeobox 1 (ZEB1) and N-cadherin and a significant decrease in the expression of zonula occludens-1 (ZO-1) in SW480 cells co-cultured with culture supernatants from tumor cell-derived exosome-pretreated THP-1-derived macrophages compared with those in the normal supernatant group (PBS-treated). In contrast, compared with those in the NC group, ZEB1, and N-cadherin expression were significantly lower, and ZO-1 expression was significantly greater in SW480 cells co-cultured with culture supernatant from THP-1-derived macrophages pretreated with exosomes from the si-circPOLQ group (figure 4G). The above results suggest that circPOLQ

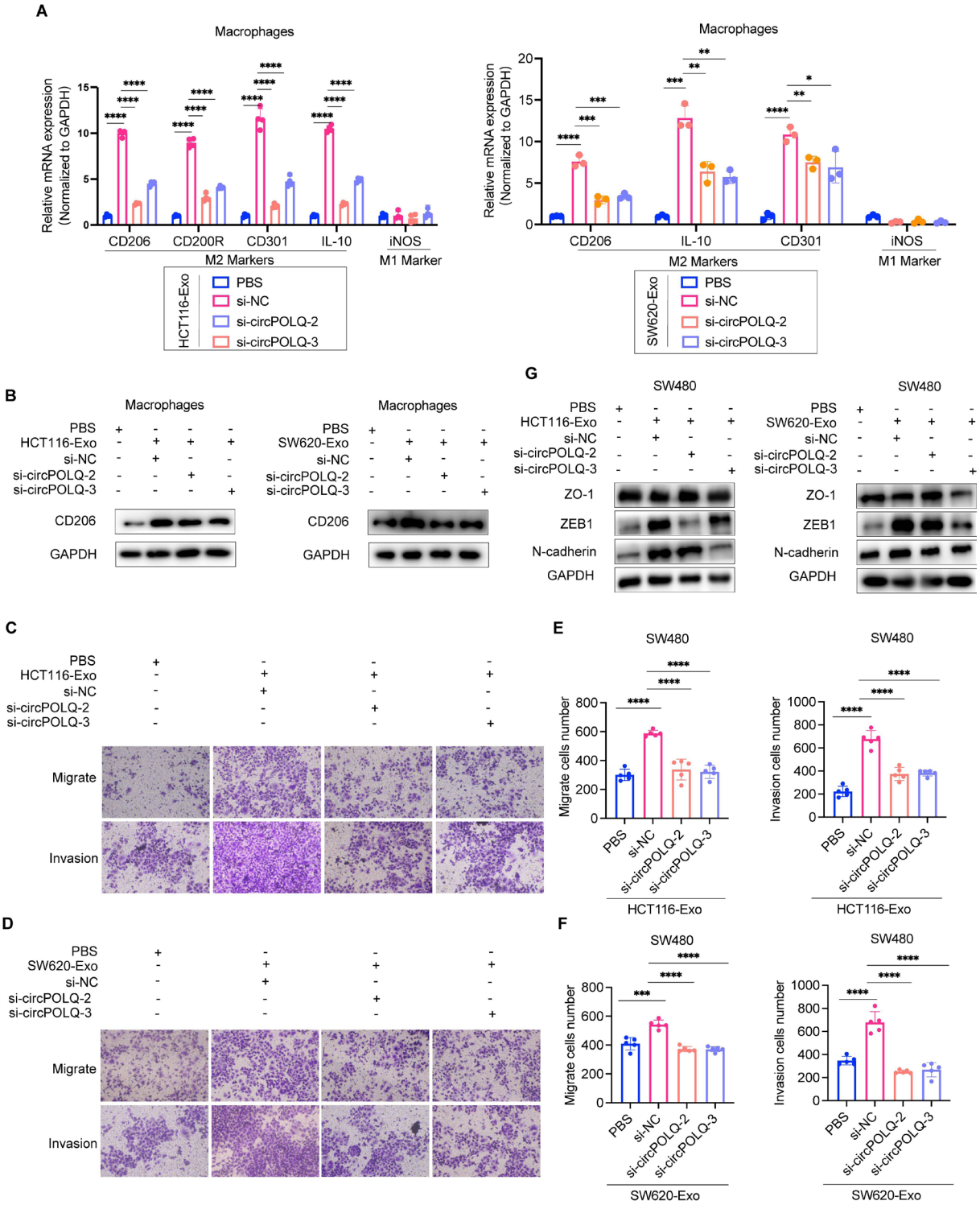

Figure 4 The exosomal circPOLQ induces macrophage M2 polarization, consequently promoting tumor cell migration and invasion. (A) Quantitative PCR analysis of the expression of typical M2 markers (CD206, CD301, CD200R and IL-10) and M1 marker (iNOS) in PMA-pretreated THP-1 cells treated with different HCT116, SW620 exosomes or PBS (control). (B) Western blot analysis of the expression of typical M2 marker CD206 in PMA-pretreated THP-1 cells treated with different HCT116, SW620 exosomes or PBS (control). (C, D) The CRC cell line SW480 was co-cultured for 12 hours with CM from PMA-treated THP-1 cells (THP-1 cells were pretreated with exosomes from differently treated CRC cells). (E, F) Effects of exogenous circPOLQ on the migration and invasion abilities of SW480. (G) The expression of epithelial-mesenchymal transition-related molecules was detected by western blot after CRC cell line SW480 was co-cultured with CM from PMA-treated THP-1 cells for 12 hours (THP-1 cells were pretreated with exosomes from differently treated CRC cells). Statistical significance was calculated by Student's t-test. Data in the text were expressed as mean±SD, *p<0.05, **p<0.01, ***p<0.001, ****p<0.0001. CM, conditioned medium; CRC, colorectal cancer; IL, interleukin; mRNA, messenger RNA; PBS, phosphate-buffered saline; PMA, phorbol 12-myristate 13-acetate; ZEB1, zinc finger E-box binding homeobox 1; ZO-1, zonula occludens-1.

enhances M2 macrophage polarization through CRC cell-derived exosomes, thereby potentially promoting tumor metastasis.

Exosomal circPOLQ promotes M2 macrophage polarization by targeting miR-379-3p in macrophages

To further investigate the mechanism by which exosomal circPOLQ affects M2 macrophage polarization, we analyzed the potential microRNAs (miRNAs) targeted by circPOLQ identified by previous sequencing analyses and identified 398 miRNAs.[20] First, we further predicted the potential miRNAs targeted by circPOLQ by bioinformatics analysis using the RegRNA website. From the Venn diagram, we selected 22 miRNAs for further study (figure 5A). Through Gene Expression Omnibus (GEO) database analysis, we revealed that miR-379–3 p expression was significantly decreased in CRC tissues (online supplemental figure 5A). Hence, we hypothesized that circPOLQ promotes M2 macrophage polarization by targeting miR-379–3 p after entry into macrophages via tumor cell-derived exosomes. To validate this hypothesis, three groups of circPOLQ luciferase reporter vectors were generated: a blank group (psiCHECK-2 vector), a wild-type group (psiCHECK-2-circPOLQ-WT), and a mutant group (psiCHECK-2-circPOLQ-MT) with a mutation in the putative miR-379–3 p binding site. Consistent with our expectations, the co-transfection of the wild-type circPOLQ vector (psiCHECK-2-circPOLQ-WT) with the miR-379–3 p mimic led to a substantial decrease in luciferase activity in 293 T cells. Conversely, co-transfection of the mutant circPOLQ vector (psiCHECK-2-circPOLQ-MT) with the miR-379–3 p mimic had no significant effect on luciferase activity ($p<0.01$) (figure 5B,C). Furthermore, we synthesized biotin-labeled probes targeting miR-379–3 p. These miR-379–3 p probes were enriched with circPOLQ, as shown by the RNA pulldown assay (figure 5D and online supplemental figure 5B). Subsequently, we examined miRNA expression in normal cultured M0 macrophages and macrophages pretreated with HCT116 cell-derived exosomes. The expression of miR-379–3 p was significantly decreased relative to that in the PBS group. In addition, we evaluated the expression of miR-379–3 p in macrophages pretreated with exosomes from HCT116 cells with circPOLQ knockdown. The expression of miR-379–3 p was significantly greater in the circPOLQ-knockdown group than in the NC group (figure 5E). The above results suggested that exosomal circPOLQ targets miR-379–3 p after entry into macrophages.

We next explored whether circPOLQ affects M2 macrophage polarization by targeting miR-379–3 p. Knockdown of miR-379–3 p reversed the effect of circPOLQ on the expression of M2 polarization markers (figure 5F,G). In addition, we isolated exosomes from the culture supernatant of HCT116 cells overexpressing circPOLQ and incubated them with M0 macrophages for 48 hours. Overexpression of miR-379–3 p diminished the effect of circPOLQ overexpression on the expression of M2 polarization markers (online supplemental figure 5C). In line with these observations, western blot analysis was performed to assess the expression of M2 macrophage markers (figure 5H,I). The results obtained from this analysis agreed with previous findings (figure 5F,G). Taken together, the above results suggested that CRC cell-derived exosomal circPOLQ affects M2 macrophage polarization by targeting miR-379–3 p after entry into macrophages.

We investigated whether downregulating miR-379–3 p may reverse the circPOLQ-induced induction of M2 macrophage polarization, which could further affect CRC metastasis. We co-cultured the hypermetastatic CRC cell line SW480 with supernatants from macrophages subjected to different treatments as described above. Downregulation of miR-379–3 p restored the migration and invasion abilities of co-cultured SW480 cells by reversing the inhibition of M2 macrophage polarization induced by circPOLQ (figure 5J–M). We then similarly examined the changes in the expression of EMT-related molecules in SW480 cells co-cultured with different exosome-treated and transfected macrophages by western blotting. Similarly, downregulation of miR-379–3 p reversed the suppression of the EMT-related molecules ZEB1 and α-SMA induced by circPOLQ downregulation and promoted the expression of the EMT-related molecules ZO-1 and E-cadherin (figure 5N,O). In conclusion, our results suggested that the CRC cell-derived exosomal circPOLQ drives M2 macrophage polarization by targeting miR-379–3 p and enhancing the migration and invasion of tumor cells.

miR-379-3p inhibits M2 polarization of macrophages, thereby suppressing tumor cell migration and invasion

We further investigated whether miR-379–3 p affects M2 macrophage polarization. Following the overexpression of miR-379–3 p, there was a substantial decrease in the expression of M2 macrophage polarization markers, including CD206, CD200R, and CD301, compared with that in the control group. Conversely, on inhibition of miR-379–3 p, the expression of the M2 macrophage polarization markers CD206 and CD200R further increased (figure 6A–F and online supplemental figure 5D–F). The above results suggested that miR-379–3 p inhibited the M2 polarization of macrophages.

Subsequently, we proceeded to examine whether the impact of miR-379–3 p on M2 macrophage polarization, induced by tumor cell-derived exosomes, had a similar influence on CRC cell migration and invasion. We induced M2 macrophage polarization using exosomes extracted from HCT116 and SW620 CRC cells. Subsequently, after transfection with the miR-379–3 p mimic or inhibitor, the weakly metastatic CRC cell line SW480 was co-cultured with conditioned medium (CM) from the above cells. Transwell assays showed that co-culture of SW480 cells with M2 macrophage CM increased the numbers of migrating and invading cells compared with those in the group without M2 macrophage CM treatment (the PBS group). In contrast, after co-culture with

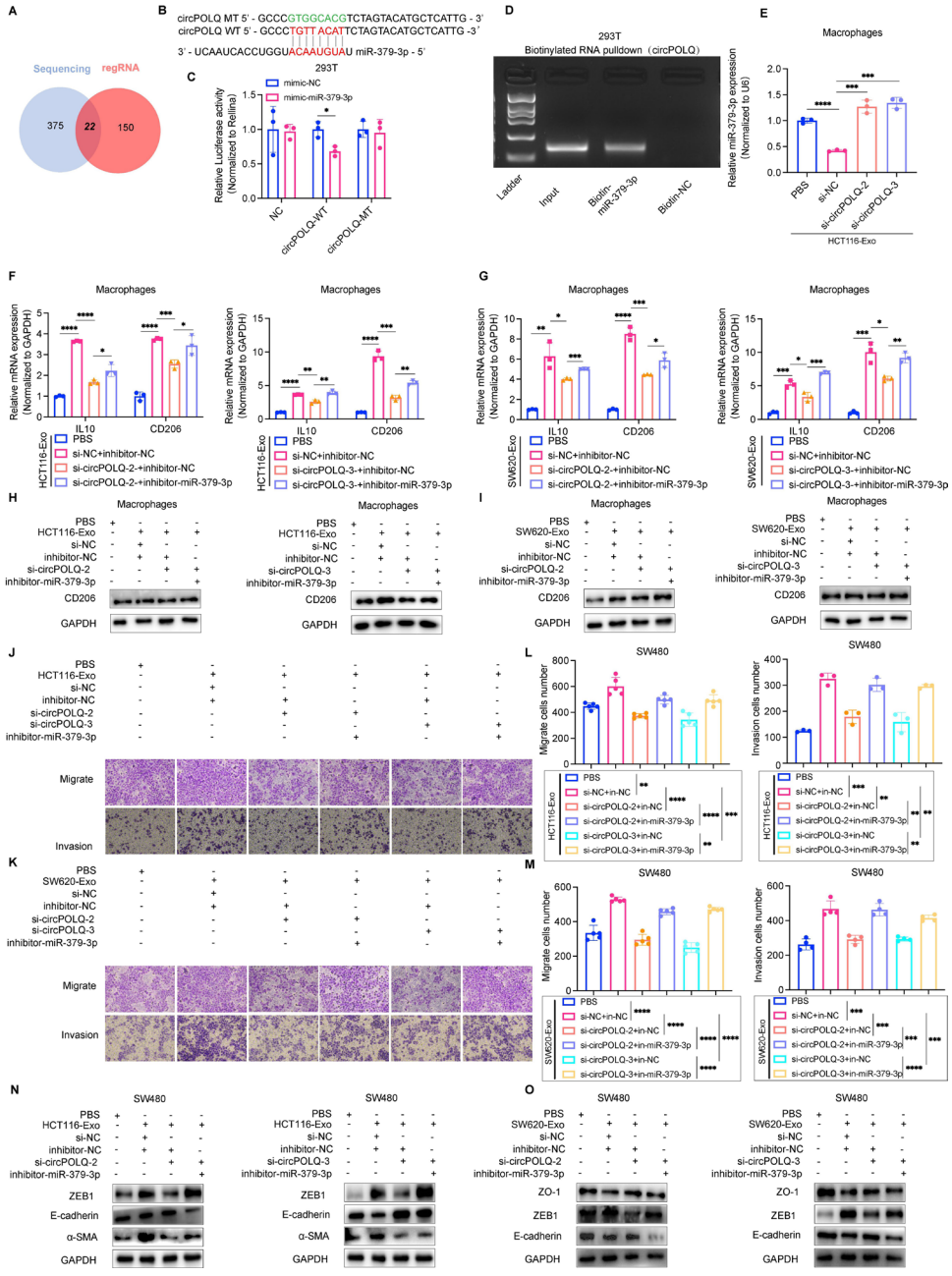

Figure 5 The exosomal circPOLQ promotes macrophage M2 polarization by targeting miR-379–3 p. (A) The intersection of six pairs of circPOLQ-targeted miRNAs predicted from colorectal cancer tissue sequencing data and circPOLQ-targeted miRNAs predicted by bioinformatics website RegRNA were screened by Venn diagram. (B) The binding site of circPOLQ to miR-379–3 p and the mutated site sequence in circPOLQ MT. (C) A luciferase reporter gene activity assay was performed to determine the effect of the miR-379–3 p mimic on the luciferase activity of WT/MT circPOLQ. (D) RNA pull-down was performed in 293 T cells, followed by qPCR and nucleic acid electrophoresis to detect the enrichment of circPOLQ. (E) Expression of miR-379–3 p detected by qPCR in macrophages treated with HCT116 cell-derived exosomes. (F, G) In macrophages treated with HCT116 or SW620 cell-derived exosomes expressing different levels of circPOLQ, transfected with miR-379–3 p inhibitor, the expression of macrophage M2 polarization markers were detected by qPCR. (H, I) In macrophages treated with HCT116 or SW620 cell-derived exosomes expressing different levels of circPOLQ, transfected with miR-379–3 p inhibitor, the expression of macrophage M2 polarization markers were detected by western blot. (J, K) The colorectal cancer cell line SW480 was co-cultured for 12 hours with CM from PMA-treated THP-1 cells (THP-1 cells were pretreated with differently treated HCT116 and SW620 exosomes). (L, M) Effects of exogenous circPOLQ on the migration and invasion abilities of SW480. (N, O) The expression of epithelial-mesenchymal transition-related molecules was detected by western blot after SW480 was co-cultured with CM from PMA-treated THP-1 cells for 12 hours (THP-1 cells were pre-treated with exosomes from differently treated colorectal cancer cells). Statistical significance was calculated by the Student's t-test. Data in the text were expressed as mean±SD, *p<0.05, **p<0.01, ***p<0.001, ****p<0.0001. CM, conditioned medium; IL, interleukin; miRNAs, microRNAs; mRNA, messenger RNA; PBS, phosphate-buffered saline; PMA, phorbol 12-myristate 13-acetate; qPCR, quantitative PCR; ZEB1, zinc finger E-box binding homeobox 1; ZO-1, zonula occludens-1.

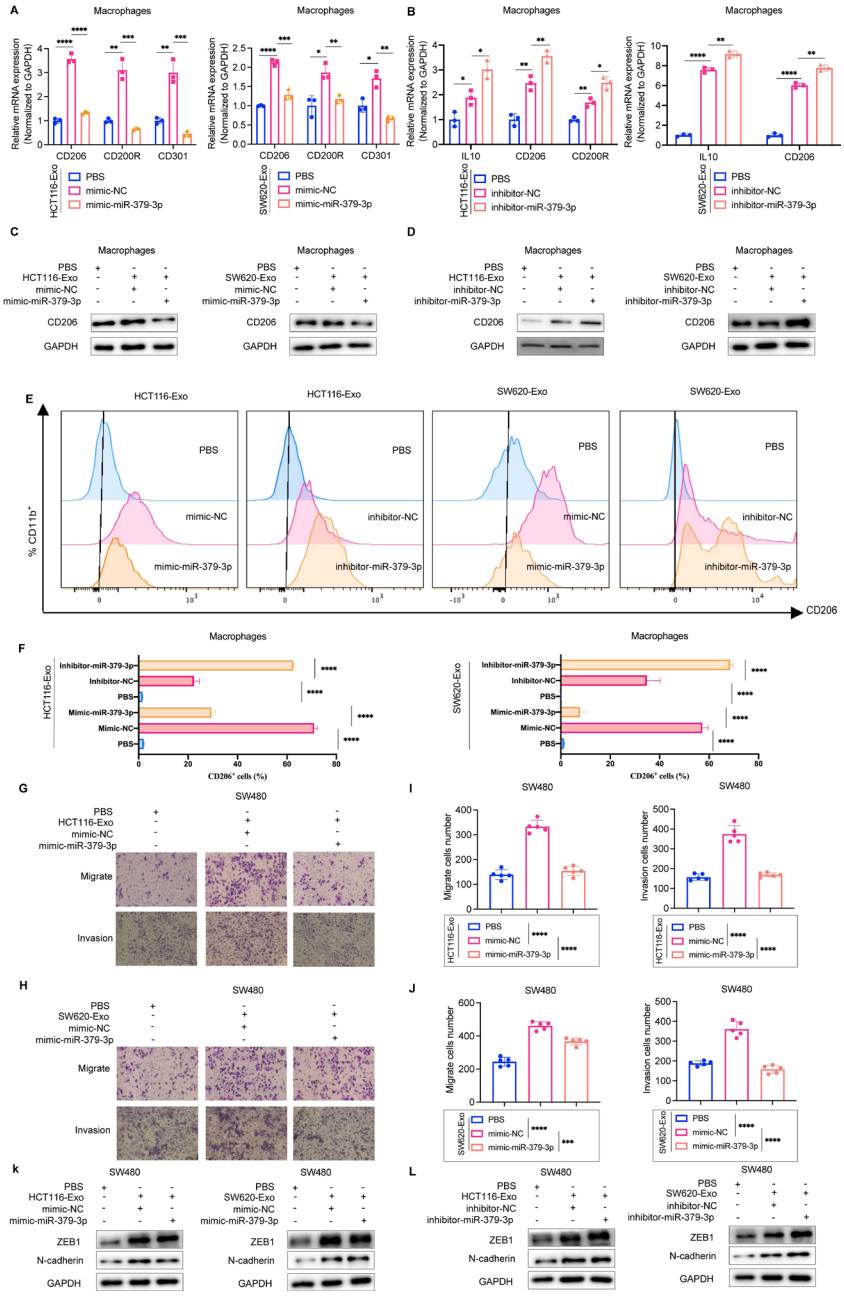

Figure 6 miR-379–3p inhibits M2 macrophage polarization, thereby enhancing tumor cell migration and invasion in vitro. (A) Macrophages treated with HCT116 and SW620 exosomes were transfected with miR-379–3p mimic, and the expression of macrophage M2 polarization markers was detected by qPCR. (B) Macrophages treated with HCT116 and SW620 exosomes were transfected with miR-379–3p inhibitor, and the expression of macrophage M2 polarization markers was detected by qPCR. (C) Macrophages treated with HCT116 and SW620 exosomes were transfected with miR-379–3p mimic, and the expression of macrophage M2 polarization marker CD206 was detected by western blot. (D) Macrophages treated with HCT116 and SW620 exosomes were transfected with miR-379–3p inhibitor, and the expression of macrophage M2 polarization marker CD206 was detected by western blot. (E) Macrophages treated with HCT116 and SW620 exosomes were transfected with miR-379–3p mimic or inhibitor, and the expression of CD206 was detected by FACS. (F) Macrophages treated with HCT116 and SW620 exosomes were transfected with miR-379–3p mimic or inhibitor, and the positive rate of CD206 was measured by FlowJo. (G, H) The CRC cell line SW480 was co-cultured for 12 hours with CM from PMA-treated THP-1 cells (THP-1 cells were pretreated with differently treated HCT116 and SW620 exosomes). (I, J) Effects of exogenous circPOLQ on the migration and invasion abilities of SW480. (K, L) The expression of epithelial-mesenchymal transition-related molecules was detected by western blot after the CRC cell line SW480 was co-cultured with CM from PMA-treated THP-1 cells for 12 hours (THP-1 cells were pretreated with exosomes from differently treated colorectal cancer cells). Statistical significance was calculated by Student's t-test. Data in the text are expressed as mean±SD, *p<0.05, **p<0.01, ***p<0.001, ****p<0.0001. CM, conditioned medium; CRC, colorectal cancer; IL, interleukin; FACS, fluorescence activated cell sorting; mRNA, messenger RNA; PBS, phosphate-buffered saline; PMA, phorbol 12-myristate 13-acetate; qPCR, quantitative PCR; ZEB1, zinc finger E-box binding homeobox 1.

CM from macrophages transfected with the miR-379–3p mimic, the numbers of migrating and invading SW480 cells were significantly lower than those in the NC group (figure 6G–J). We also measured the expression of the EMT-related molecules ZEB1 and by protein immunoblotting, and the results were consistent with the above trends (figure 6K,L).

In brief, our results showed that miR-379–3p inhibits M2 macrophage polarization and thus suppresses tumor cell migration and invasion.

Exosomal circPOLQ promotes M2 macrophage polarization via the miR-379-3p/IL-10/signal transducer and activator of transcription 3 axis

We further explored the potential mechanisms by which circPOLQ affects M2 macrophage polarization. We used the TargetScan Human 7.2 database to predict the possible messenger RNAs (mRNAs) targeted by miR-379–3p. The results showed that miR-379–3p has a high potential to target IL-10 (figure 7A). Analysis of data from The Cancer Genome Atlas demonstrated that high expression of IL-10 was closely correlated with poorer disease-specific survival in patients with CRC (online supplemental figure 6A). In addition, analysis of the GSE87211 data set in the GEO database similarly showed that high expression of IL-10 was significantly correlated with poorer survival in patients with CRC (online supplemental figure 6B). Furthermore, IL-10 was associated with macrophage activation, as determined by Gene Set Enrichment Analysis (online supplemental figure 6C). These data suggested that miR-379–3p might target IL-10 to induce M2 macrophage polarization. To confirm the targeting of IL-10 by miR-379–3p, we generated three IL-10 luciferase reporter vectors: a blank vector (psiCHECK-2), a wild-type vector (psiCHECK-2-IL-10-WT), and a mutant vector (psiCHECK-2-IL-10-MT) with a mutation introduced in the putative miR-379–3p binding site. As expected, co-transfection of psiCHECK-2-IL-10-WT but not psiCHECK-2-IL-10-MT with the miR-379–3p mimic significantly reduced luciferase activity in 293T cells ($p<0.01$) (figure 7B). Additionally, through an RNA pulldown assay, we constructed a biotin-labeled probe targeting miR-379–3p and found that IL-10 was significantly enriched by in the miR-379–3p-treated 293T cells (figure 7C). The above results suggested that miR-379–3p targets IL-10.

Furthermore, we constructed si-IL-10 and IL-10 overexpression (lv-IL-10) plasmids and verified the reliability of si-IL-10 and lv-IL-10 (online supplemental figure 6D). We transfected the miR-379–3p mimic or inhibitor into macrophages pretreated with tumor cell-derived exosomes and detected changes in IL-10 expression by qPCR. We detected a significant decrease in macrophage IL-10 expression after miR-379–3p overexpression compared with that in the control group, while miR-379–3p knockdown resulted in a significant increase in macrophage IL-10 expression (online supplemental figure 6D). These findings further demonstrated that miR-379–3p regulated the mRNA level of IL-10. Moreover, we co-transfected the miR-379–3p mimic and si-IL-10 or the miR-379–3p inhibitor and Lv-IL-10 into macrophages pretreated with tumor cell-derived exosomes. The qPCR results demonstrated that IL-10 reversed the impact of miR-379–3p on M2 macrophage polarization (figure 7D,E). These results suggested that miR-379–3p suppresses the M2 polarization of macrophages by targeting IL-10. Transwell assays showed that after co-culture with CM from macrophages transfected with the miR-379–3p inhibitor, the numbers of migrating and invading SW480 cells were significantly greater than those in the NC group, and si-IL-10 significantly reversed these effects (online supplemental figure 7A–D). We then similarly examined the variation in the expression of EMT-related molecules in SW480 cells co-cultured with different exosome-treated and transfected macrophages by western blotting. Consistent with the above findings, overexpression of IL-10 reversed the miR-379–3p overexpression-mediated inhibition of the expression of the EMT-related molecules ZEB1 and N-cadherin (online supplemental figure 7E). Knockdown of IL-10 reversed the miR-379–3p inhibition-induced increase in the expression of the EMT-related molecules ZEB1 and N-cadherin (online supplemental figure 7F).

Activation of the signal transducer and activator of transcription 3 (STAT3) signaling pathway plays a crucial role in M2 polarization of macrophages, thereby facilitating tumor progression.[34 35] IL-10 acts as a positive regulator of the STAT3 signaling pathway and has been demonstrated to regulate the process of M2 macrophage polarization.[36] Kyoto Encyclopedia of Genes and Genomes pathway enrichment analysis revealed that IL-10 was significantly related to the JAK/STAT signaling pathway (online supplemental figure 8A). Therefore, we hypothesized that tumor cell-derived exosomal circPOLQ affects M2 polarization of macrophages through the STAT3 signaling pathway via IL-10. To verify this hypothesis, we incubated macrophages with exosomes from circPOLQ-knockdown tumor cells and then measured the level of phosphorylated STAT3 (p-STAT3) by western blotting. The level of p-STAT3 was significantly lower in macrophages cultured with exosomes from tumor cells stimulated with circPOLQ knockdown plasmid than in those from control macrophages (figure 7F). Subsequently, based on these results, we further knocked down the expression of miR-379–3p and found that miR-379–3p reversed the decrease in the level of p-STAT3 (figure 7G and online supplemental figure 8B).

In addition, we transfected mimics or inhibitors of miR-379–3p into macrophages pretreated with tumor cell-derived exosomes to investigate the activation of the STAT3 pathway. Similarly, the changes in the level of p-STAT3 and the expression of the M2 macrophage marker CD206 were similarly reversed by IL-10 modulation, as determined by western blot analysis after knockdown or overexpression of IL-10 (figure 7H,I and online supplemental figure 8C,D).

We next further explored the mechanism by which circPOLQ affects M2 macrophage polarization via the

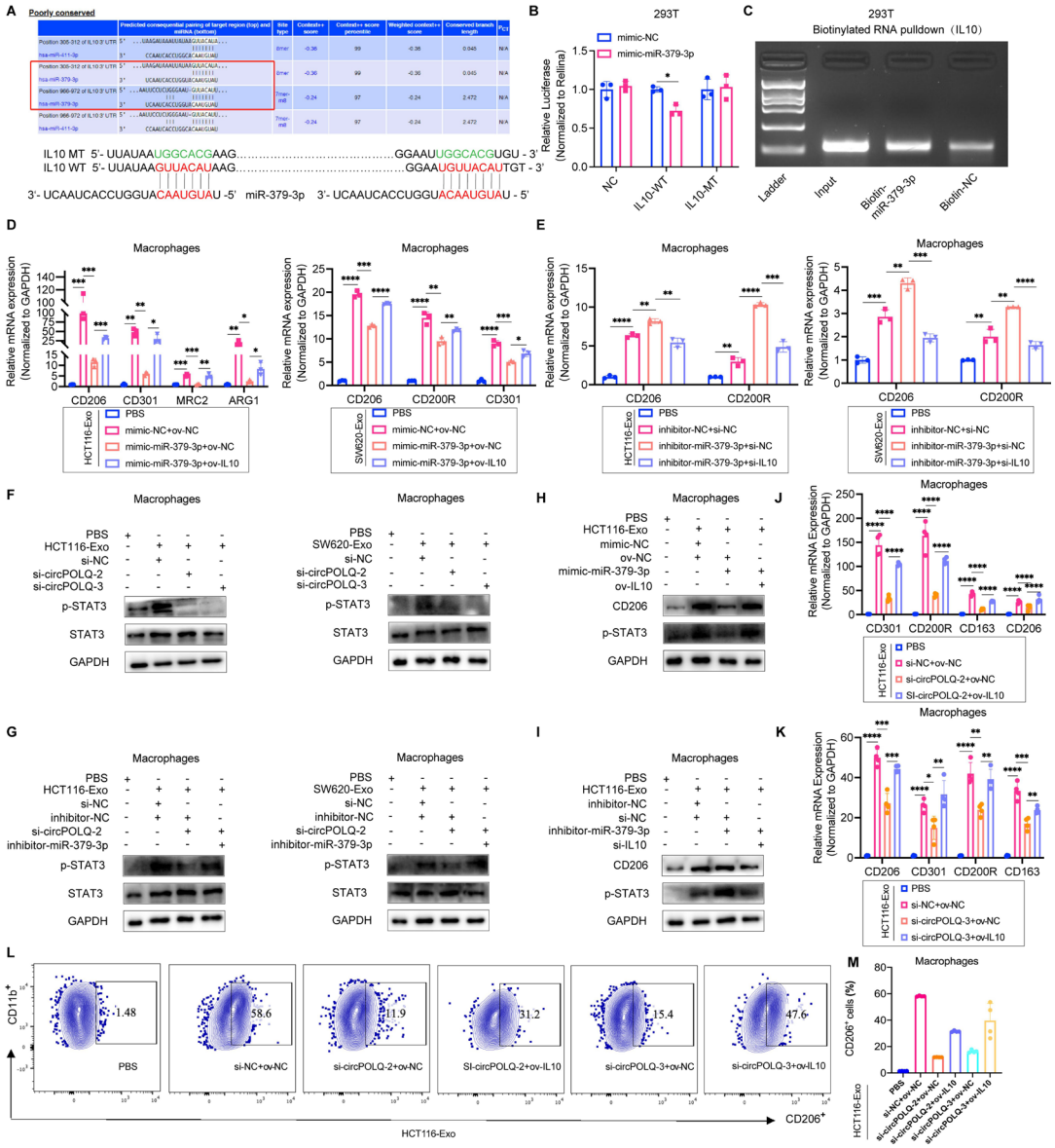

Figure 7 Exosomal circPOLQ induces macrophage M2 polarization through the mir-379–3p/IL-10/STAT3 axis. (A) TargetScan Human V.7.2 database predicts that miR-379–3p may target the binding site of IL-10 and the mutation site of IL-10 MT. (B) A luciferase reporter gene activity assay was performed to determine the effect of the miR-379–3p mimic on the 3'-UTR luciferase activity of WT/MT IL-10. (C) RNA pull-down was performed in 293T cells, followed by qPCR and nucleic acid electrophoresis to detect the enrichment of IL-10. (D) Macrophages treated with HCT116 or SW620 exosomes were co-transfected with miR-379–3p mimics and IL-10-overexpressing plasmids, and the expression of macrophage M2 polarization markers was detected by qPCR. (E) Macrophages treated with HCT116 or SW620 exosomes were co-transfected with miR-379–3p inhibitor and IL-10 siRNA, and the expression of macrophage M2 polarization markers was detected by qPCR. (F) Macrophages treated with HCT116 or SW620 exosomes were transfected with circPOLQ siRNA, and the expressions of p-STAT3 and STAT3, key molecules of STAT3 signaling pathway, were detected by western blot. (G) Macrophages treated with HCT116 or SW620 exosomes were co-transfected with circPOLQ siRNA and miR-379–3p inhibitor, and the expressions of p-STAT3 and STAT3, key molecules of STAT3 signaling pathway, were detected by western blot. (H) Macrophages treated with HCT116 exosomes were co-transfected with miR-379–3p mimics and overexpressed IL-10 plasmids, and the key molecules of STAT3 signaling pathway p-STAT3 and macrophage M2 polarization markers were detected by western blot. (I) Macrophages treated with HCT116 exosomes were co-transfected with miR-379–3p inhibitor and IL-10 siRNA, and the key molecules of STAT3 signaling pathway p-STAT3 and macrophage M2 polarization markers were detected by western blot. (J, K) Macrophages treated with HCT116 exosomes were co-transfected with circPOLQ siRNA and overexpressed IL-10 plasmids, and the expression of macrophage M2 polarization markers was detected by qPCR. (L, M) Macrophages treated with HCT116 exosomes were co-transfected with circPOLQ siRNA and overexpressed IL-10 plasmids, and the expression of CD206 was detected by FACS and the positive rate of CD206 was measured by FlowJo. Statistical significance was calculated by Student's t-test. Data in the text were expressed as mean±SD, *p<0.05, **p<0.01, ***p<0.001, ****p<0.0001. FACS, fluorescence activated cell sorting; IL, interleukin; mRNA, messenger RNA; PBS, phosphate-buffered saline; p-STAT3, phosphorylated signal transducer and activator of transcription-3; qPCR, quantitative PCR; STAT3, signal transducer and activator of transcription 3.

IL-10/STAT3 axis. Compared with that in control macrophages, the expression of IL-10 in macrophages treated with exosomes derived from tumor cells with circPOLQ knockdown was significantly lower, while a significant increase in IL-10 expression occurred after the overexpression of IL-10 (online supplemental figure 8E). Subsequently, we evaluated the expression levels of M2 macrophage polarization markers and observed a notable increase in their expression concurrent with the upregulation of IL-10 (figure 7J–M and online supplemental figure 8F).

In summary, these data collectively indicate that tumor cell-derived exosomal circPOLQ stimulates M2 macrophage polarization through the miR-379–3p/IL-10/STAT3 axis.

Exosomal circPOLQ promotes CRC cell metastasis by inducing M2 macrophage polarization in vivo

To further evaluate the role of exosomal circPOLQ in inducing M2 macrophage polarization and thus promoting CRC progression in vivo, we collected supernatants from THP-1 macrophages which had been incubated for 48 hours with HCT116 derived circPOLQ containing exosomes or control exosomes, respectively, and subsequently co-cultured luci expressing SW480 cell line with the harvested supernatants for 72 hours. Considering that the liver and lungs are common targets for CRC metastasis, we injected the in vitro-prepared SW480 cell line into NSG mice via the spleen and tail vein to establish models of CRC liver and lung metastases (online supplemental figure 9A). At 30 days after injection, in vivo fluorescence imaging of the NSG mice injected intrasplenically with SW480 cells cultured with exosomes overexpressing circPOLQ in vitro revealed stronger fluorescence at liver nodules, whereas the control mice had more in situ splenic carcinomas (online supplemental figure 9B). Subsequently, the NSG mice were euthanized, and liver and lung tissues were removed for H&E staining. The group of mice in which the SW480 model group was cultured in vitro with exosomes overexpressing circPOLQ had more and larger liver and lung nodules (online supplemental figure 9CF, I, and L). We evaluated the expression of EMT-related molecules in liver and lung nodules by immunohistochemistry (online supplemental figure 9D,E,J and K) and found a significant increase in the proportion of the number of cells positive for the EMT-related molecules vimentin (VIM) and N-cadherin (online supplemental figure 9G,H,M and N). These findings imply that the CRC cell-derived exosomal circPOLQ promotes the nodule formation of CRC in vivo by inducing M2 macrophage polarization.

To further verify that exosome-derived circPOLQ crosstalk tumor cells and macrophages promote CRC metastasis in vivo, we established an orthotopic CRC metastasis model by colonizing the cecum of NSG mice,[21] with an equal mixture of HCT116 stably overexpressing circPOLQ or control cells and mature macrophages induced by PMA[24] (figure 8A). In vivo fluorescence imaging revealed that mice in the circPOLQ overexpression group exhibited early intense fluorescence in the liver, whereas the control group showed limited fluorescence confined to the lower abdomen (figure 8B). The experiment was terminated after 6 weeks. In situ tumors, compared with the control group, the cancer cells in the circPOLQ overexpression group exhibited high expression of EMT molecules VIM and N-cadherin (figure 8C–E), while the levels of CD163 and CD206 in macrophages were significantly elevated (figure 8F–H). In addition, the number of metastases in distant organs, such as the liver and lungs, in the circPOLQ overexpression group was significantly higher than that in the control group (figure 8I–K). The above in vitro and in vivo experiments above strongly suggested that CRC cell-derived exosomal circPOLQ could enter macrophages and target miR-379–3p to further promote the activation of the IL-10/STAT3 axis, thereby inducing the polarization of macrophages to the M2 phenotype. CRC cell-derived circPOLQ induced M2-type macrophages, which further enhanced CRC metastasis (figure 8L).

DISCUSSION

Although some progress in CRC treatment has been made, distant metastasis of CRC still poses a serious threat to the health of patients with CRC and is the main reason for their low long-term survival rate. Tumor metastasis refers to the intricate process by which tumor cells originating from the primary site disseminate to remote organs and tissues, leading to the formation of secondary tumors. Current studies suggest that immune cells in the TME are essential and critical factors in the process of tumor metastasis. During the early stages of tumor formation, immune cells, particularly those with cytotoxic effects, have the ability to identify and eliminate highly immunogenic tumor cells.[37] However, as a result of tumor heterogeneity, a subpopulation of cancer cells might exhibit decreased immunogenicity, enabling them to evade immune recognition and immune cell-mediated elimination. Furthermore, tumor cells can drive the differentiation of immune cells infiltrating tumors toward a phenotype that supports tumor growth and progression[38]; moreover, TAMs are particularly affected by these cells. In our study, we found that co-culture of TAMs with low metastatic CRC cells significantly increased the migration and invasion ability of CRC cells. Clinical data show a significant correlation between a high level of macrophage infiltration and poor prognosis.[39] However, the mechanism by which tumor cells reprogram infiltrating macrophages and the impact of reprogrammed macrophages on tumor progression are unclear.

Macrophages have diverse functions and even have completely opposite phenotypes in different environments. TAMs mainly exhibit an M2-like phenotype and exhibit immunosuppressive and tumor progression-promoting effects. Targeting M2-like TAMs and either depleting them within the TME or reprogramming them

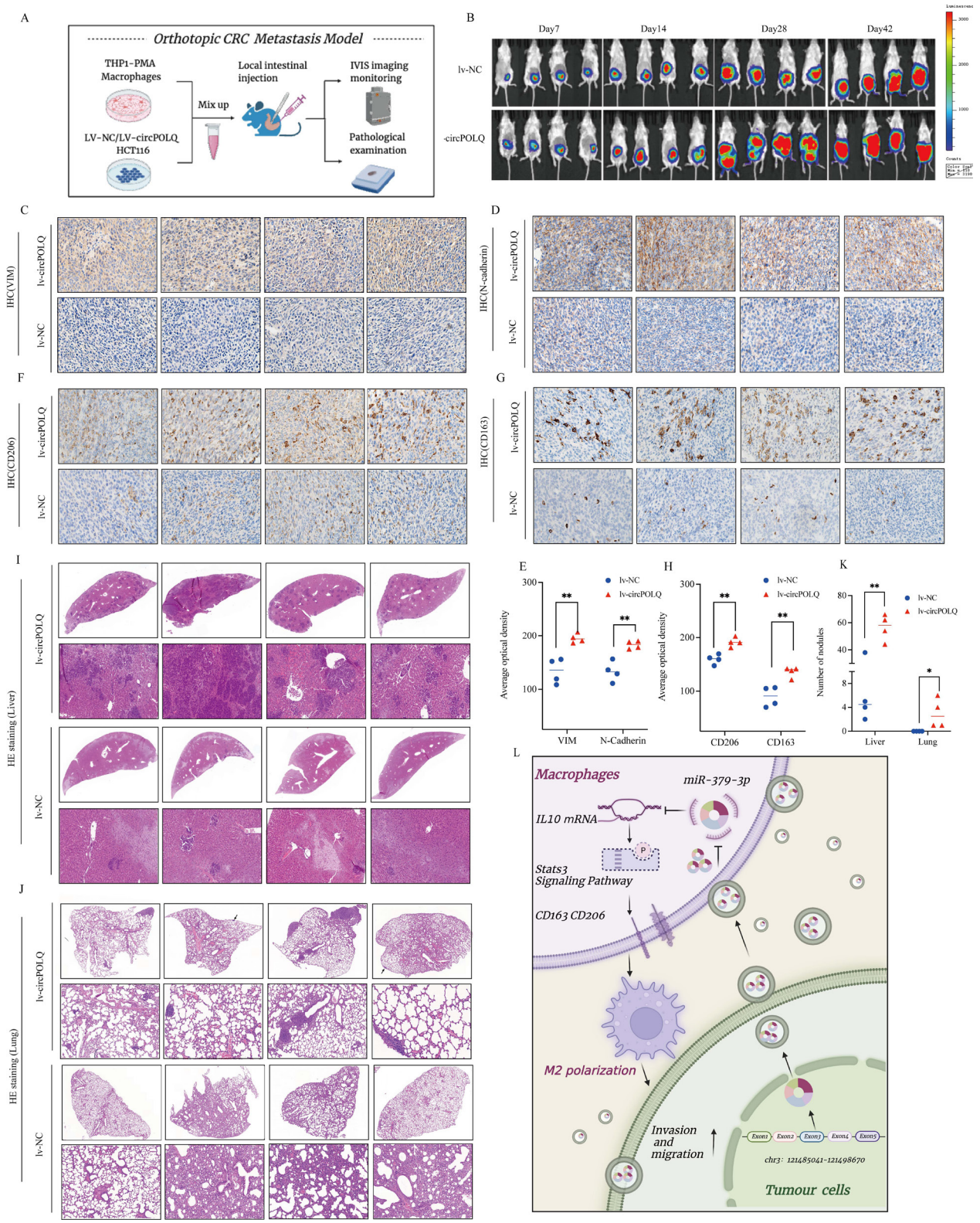

Figure 8 The tumor-derived exosome circPOLQ promotes CRC cell metastasis by inducing macrophage M2 polarization in vivo. (A) Flow chart of orthotopic CRC metastasis animal model. (B) In vivo fluorescence imaging of intestinal tumors and metastasis in NSG mice at regular intervals. (C, D) IHC analysis of epithelial-mesenchymal transition-related molecules VIM and N-cadherin in NSG mice with carcinoma in situ. (E) The average optical density of VIM and N-cadherin. (F, G) IHC analysis of macrophage M2 polarization-related molecules CD206 and CD163 in NSG mice with carcinoma in situ. (H) The average optical density of CD206 and CD163. (I) H&E staining of the livers of four pairs of NSG mice. (J) H&E staining of the lungs of four pairs of NSG mice. (K) The number of nodules in the livers and lungs of NSG mice. (L) Graphical outline of the proposed mechanism in this study. Statistical significance was calculated by the Student's t-test. Data in the text were expressed as mean±SD, *p<0.05, **p<0.01. CRC, colorectal cancer; IHC, immunohistochemistry; VIM, vimentin.

toward an M1-like phenotype are potential strategies to enhance their cytotoxicity directly and indirectly by stimulating cytotoxic T cells to eliminate tumor cells. These approaches hold promise as potential therapeutic strategies for antitumor immunotherapy. However, the mechanism by which tumor cells reprogram macrophages into TAMs to promote tumor metastasis progression is unclear. Several studies have reported that tumor cells can secrete various cytokines that can directly induce the polarization of macrophages into TAMs. In this study, we detected significant upregulation of macrophage surface molecules such as CD206, CD301, and CD200R after co-culturing CRC cell line culture supernatant with macrophages. Similarly, when tumor cells were co-cultured with macrophages, the expression of IL-10, IL-12, IL-6, TNF, CCL5, CCL22, and CSF1 was upregulated, leading to M2 polarization of macrophages.[40] Moreover, tumor cells can generate metabolic byproducts that influence the functionality of immune cells infiltrating the TME, thereby fostering the progression of tumor cells. For instance, it has been reported that tumor cells release succinate into their microenvironment, which then activates succinate receptor signaling. This signaling pathway plays a role in polarizing macrophages toward the TAM phenotype.[41] Furthermore, studies have revealed that all-trans retinoic acid can effectively hinder osteosarcoma metastasis by inhibiting the M2 polarization of TAMs.[30]

Exosomes are extracellular carriers that have a diameter of 30–150 nm and contain proteins, RNA, lipids, DNA, etc. Moreover, a growing body of evidence has demonstrated that tumor cell-derived exosomes, in various types of cancer, can be released into the TME to modulate the functions of immune cells in various types of cancer. This phenomenon results in the creation of a more conducive environment for tumor development.[42] Exosomes derived from tumor cells reportedly promote immune escape and malignant progression of tumor cells by downregulating NKG2D on the surface of natural killer (NK) cells and causing a significant decrease in NK cell toxicity.[43] Studies have shown that treatment of adipocytes with hepatocellular carcinoma-derived exosomes activates several phosphokinase and nuclear factor kappa-B (NF-κB)signaling pathways in adipocytes, which in turn creates a favorable microenvironment for tumors.[44] Furthermore, tumor-derived exosomes play a crucial role in modulating the polarization of macrophages. It has been reported that tumor cell-derived exosomes influence the metabolic reprogramming of macrophages through NF-kB-dependent glycolysis, leading to increased expression of programmed cell death 1 ligand 1 (PD-L1). This ultimately polarizes macrophages toward an immunosuppressive phenotype.[45] Exosomal RNAs include mRNAs and non-coding RNAs. Currently, the exploration of tumor-derived exosomal non-coding RNAs involved in M2 macrophage polarization has focused mostly on miRNAs and long non-coding RNAs (lncRNAs). For instance, various studies have reported that tumor cell-derived exosomal miR-934 can induce the polarization of macrophages toward the M2 phenotype. This effect is achieved through the downregulation of PTEN expression and subsequent activation of the PI3K/AKT signaling pathway following the uptake of exosomes by macrophages.[46] Breast cancer cell-derived exosomal miR-138–5 p can enter macrophages and inhibit M1 polarization but stimulate M2 polarization by downregulating KDM6B expression.[47] The exosome lncRNA HCG18 derived from gastric cancer cells has been shown to decrease the level of miR-875–3 p in macrophages, thereby promoting M2 macrophage polarization.[48] In addition to miRNAs and lncRNAs, a novel type of non-coding RNA, circRNA, is another possible type of tumor cell-derived exosomal non-coding RNA. Numerous studies have identified circRNAs as key factors in regulating tumor progression. For example, our previous study showed that circ1662 promoted CRC progression by regulating the nucleation of YAP1.[20] However, the effects and mechanisms of tumor cell-derived exosomal circRNAs related to the TME and TAMs have not been elucidated.

In our new study, we demonstrated that exosomes secreted by CRC cells can carry circPOLQ into macrophages, target miR-379–3 p, and further regulate IL-10/STAT3 signaling pathway to induce M2 polarization. In addition, we also demonstrated that circPOLQ-enriched CRC cell-derived exosomes induced M2 macrophage polarization and finally promoted tumor cell migration and invasion in vitro and in vivo. There are a few directions in our study that require further investigation. The factors involved in the TME are very complex. Our study only explored the regulatory mechanism between tumor cells and immune cells, and it is not clear whether other types of immune cells and stromal cells play a role in it. Second, primary and metastatic nodule formation in the liver and lung were selected as the in vivo metastasis models to confirm that exosomal circPOLQ promoted CRC metastasis through the crosstalk between tumor cells and macrophages. However, this mechanism has not been verified in a large number of clinical samples, and there are opportunities for further prospective studies on CRC metastasis in the future. This still needs to be explored in new subjects.

CONCLUSIONS

In this study, we presented evidence that circPOLQ is highly expressed in both primary and metastatic CRC tissues. Importantly, its overexpression was significantly associated with poor prognosis in patients with CRC. Notably, our findings revealed that exosomes enriched with circPOLQ play a crucial role in promoting the invasion and migration of CRC cells. This effect was mediated through facilitating communication between CRC cells and TAMs, leading to the formation of a microenvironment that promotes CRC metastasis. The interaction between tumor cell-derived exosomal circPOLQ and TAMs reveals a molecular mechanism that enhances the distant metastasis of CRC.

Accumulating evidence suggests that tumor-derived exosomes commonly transfer circRNAs to recipient cells, thereby playing various functional roles.[19 49] However, studies investigating the transfer of circRNAs derived from CRC cells to macrophages, as well as their potential impact on M2 macrophage polarization are rare. Although tumor-derived exosomes can induce M2 macrophage polarization and thereby facilitate tumor cell metastasis, the specific molecular mechanism underlying the promotion of M2 macrophage polarization and tumor cell metastasis by exosomes derived from CRC cells has not been elucidated and requires further investigation. In our study, we demonstrated that circPOLQ was transferred into macrophages via CRC cell-derived exosomes. In addition, exosomal circPOLQ entered macrophages and induced M2 polarization by targeting miR-379–3p, which further regulated the IL-10/STAT3 signaling pathway. These findings align with previous reports suggesting that exosomal circRNAs can be effectively transported to target cells, thereby exerting regulatory effects on their biological functions.

The polarization of TAMs toward the M2 phenotype plays a crucial role in regulating tumor growth, migration, and angiogenesis. In this study, we provide evidence that exosomes derived from CRC cells and enriched with circPOLQ induce M2 macrophage polarization, ultimately promoting tumor cell migration and invasion.

Author affiliations
[1]Department of Colorectal Surgery, The First Affiliated Hospital of Zhengzhou University, Zhengzhou, Henan, China
[2]Henan Institute of Interconnected Intelligent Health Management, The First Affiliated Hospital of Zhengzhou University, Zhengzhou, Henan, China
[3]Academy of Medical Sciences, The First Affiliated Hospital of Zhengzhou University, Zhengzhou, Henan, China
[4]Department of Radiotherapy, Henan Cancer Hospital Affiliated Cancer Hospital of Zhengzhou University, Zhengzhou, Henan, China

Acknowledgements This work was supported by the Youth Talent Innovation Team Support Program of Zhengzhou University (32320290). Research and Innovation Team of the First Affiliated Hospital of Zhengzhou University (ZYCXTD2023017). The Provincial and Ministry Co-constructed Key Projects of Henan Medical Science and Technology (SBGJ202102134). Henan Provincial Health and Health Commission Joint Construction Project (LHGJ20200158). Henan Province Young and Middle-aged Health Science and Technology Innovation Leading Talent Project (YXKC2022016). The graphical outlines were created by BioRender.com.

Contributors ZS is the author responsible for the overall content as the guarantor. YX, ZS, BS conceptualized the whole article. ZS, YX, BS, CC designed the methods covered in the article. BS, YX, CC, PD conducted background research on the viability of the article. YX, BS visualized the experimental data of the article. PD, SH, HS supervised the entire work of the article. ZS, YX, BS wrote the original manuscript of the article. BS, YX, YL, JL, CW, JH reviewed and edited the original manuscript. All authors read and approved the final manuscript.

Funding This work was supported by the Youth Talent Innovation Team Support Program of Zhengzhou University (32320290). Research and Innovation Team of the First Affiliated Hospital of Zhengzhou University (ZYCXTD2023017). The Provincial and Ministry Co-constructed Key Projects of Henan Medical Science and Technology (SBGJ202102134). Henan Provincial Health and Health Commission Joint Construction Project (LHGJ20200158). Henan Province Young and Middle-aged Health Science and Technology Innovation Leading Talent Project (YXKC2022016). Henan Youth Health Science and Technology Innovation Leading Talents Training Project (YXKC2022004).

Competing interests None declared.

Patient consent for publication Not applicable.

Ethics approval This study was approved by the Ethics Committee of the First Affiliated Hospital of Zhengzhou University (2019-KY-423), and all patients obtained informed consent before enrollment. All mouse procedures were approved by the Animal Protection and Use Committee of Zhengzhou University (2019-KY-423).

Provenance and peer review Not commissioned; externally peer reviewed.

Data availability statement All data relevant to the study are included in the article or uploaded as supplementary information.

Supplemental material This content has been supplied by the author(s). It has not been vetted by BMJ Publishing Group Limited (BMJ) and may not have been peer-reviewed. Any opinions or recommendations discussed are solely those of the author(s) and are not endorsed by BMJ. BMJ disclaims all liability and responsibility arising from any reliance placed on the content. Where the content includes any translated material, BMJ does not warrant the accuracy and reliability of the translations (including but not limited to local regulations, clinical guidelines, terminology, drug names and drug dosages), and is not responsible for any error and/or omissions arising from translation and adaptation or otherwise.

Open access This is an open access article distributed in accordance with the Creative Commons Attribution Non Commercial (CC BY-NC 4.0) license, which permits others to distribute, remix, adapt, build upon this work non-commercially, and license their derivative works on different terms, provided the original work is properly cited, appropriate credit is given, any changes made indicated, and the use is non-commercial. See http://creativecommons.org/licenses/by-nc/4.0/.

ORCID iD
Zhenqiang Sun http://orcid.org/0000-0001-5926-2716

REFERENCES

1 Kopetz S, Chang GJ, Overman MJ, *et al*. Improved survival in metastatic colorectal cancer is associated with adoption of hepatic resection and improved chemotherapy. *J Clin Oncol* 2009;27:3677–83.
2 Bejarano L, Jordão MJC, Joyce JA. Therapeutic targeting of the tumor Microenvironment. *Cancer Discov* 2021;11:933–59.
3 Hanahan D, Coussens LM. Accessories to the crime: functions of cells recruited to the tumor Microenvironment. *Cancer Cell* 2012;21:309–22.
4 Hanahan D, Weinberg RA. Hallmarks of cancer: the next generation. *Cell* 2011;144:646–74.
5 Noy R, Pollard JW. Tumor-associated Macrophages: from mechanisms to therapy. *Immunity* 2014;41:49–61.
6 Mantovani A, Allavena P. The interaction of anticancer therapies with tumor-associated Macrophages. *J Exp Med* 2015;212:435–45.
7 Xiang X, Wang J, Lu D, *et al*. Targeting tumor-associated Macrophages to Synergize tumor Immunotherapy. *Signal Transduct Target Ther* 2021;6:75.
8 Yang H, Zhang Q, Xu M, *et al*. Ccl2-Ccr2 axis recruits tumor associated Macrophages to induce immune evasion through PD-1 signaling in Esophageal carcinogenesis. *Mol Cancer* 2020;19:41.
9 Vadevoo SMP, Gunassekaran GR, Lee C, *et al*. The macrophage Odorant receptor Olfr78 mediates the lactate-induced M2 phenotype of tumor-associated Macrophages. *Proc Natl Acad Sci U S A* 2021;118:e2102434118.
10 Wahlgren J, De L Karlson T, Brisslert M, *et al*. Plasma Exosomes can deliver exogenous short interfering RNA to monocytes and lymphocytes. *Nucleic Acids Res* 2012;40:e130.
11 Milane L, Singh A, Mattheolabakis G, *et al*. Exosome mediated communication within the tumor Microenvironment. *J Control Release* 2015;219:278–94.
12 Fan Q, Yang L, Zhang X, *et al*. The emerging role of Exosome-derived non-coding Rnas in cancer biology. *Cancer Lett* 2018;414:107–15.
13 Yang L, Peng X, Li Y, *et al*. Long non-coding RNA HOTAIR promotes Exosome secretion by regulating Rab35 and Snap23 in hepatocellular carcinoma. *Mol Cancer* 2019;18:78.
14 Li C, Ni Y-Q, Xu H, *et al*. Roles and mechanisms of Exosomal non-coding Rnas in human health and diseases. *Sig Transduct Target Ther* 2021;6:383.
15 Patop IL, Wüst S, Kadener SP. Present, and future of circRNAs. *EMBO J* 2019;38:e100836.
16 Zhou W-Y, Cai Z-R, Liu J, *et al*. Circular RNA: metabolism, functions and interactions with proteins. *Mol Cancer* 2020;19:172.
17 Chen L-L. The expanding regulatory mechanisms and cellular functions of circular Rnas. *Nat Rev Mol Cell Biol* 2020;21:475–90.

18 Kristensen LS, Jakobsen T, Hager H, *et al*. The emerging roles of circRNAs in cancer and oncology. *Nat Rev Clin Oncol* 2022;19:188–206.
19 Huang X-Y, Huang Z-L, Huang J, *et al*. Exosomal circRNA-100338 promotes hepatocellular carcinoma metastasis via enhancing Invasiveness and angiogenesis. *J Exp Clin Cancer Res* 2020;39:20.
20 Chen C, Yuan W, Zhou Q, *et al*. N6-Methyladenosine-induced Circ1662 promotes metastasis of colorectal cancer by accelerating Yap1 nuclear localization. *Theranostics* 2021;11:4298–315.
21 Tseng W, Leong X, Engleman E. Orthotopic mouse model of colorectal cancer. *J Vis Exp* 2007.:484.
22 Shi G, Yang Q, Zhang Y, *et al*. Modulating the tumor Microenvironment via Oncolytic viruses and CSF-1R inhibition synergistically enhances anti-PD-1 Immunotherapy. *Mol Ther* 2019;27:244–60.
23 Lu Z, Ortiz A, Verginadis II, *et al*. Regulation of Intercellular Biomolecule transfer-driven tumor angiogenesis and responses to anticancer therapies. *J Clin Invest* 2021;131:e144225.
24 Hadjidaniel MD, Muthugounder S, Hung LT, *et al*. Tumor-associated Macrophages promote neuroblastoma via Stat3 Phosphorylation and up-regulation of C-MYC. *Oncotarget* 2017;8:91516–29.
25 Cassetta L, Pollard JW. Tumor-associated Macrophages. *Curr Biol* 2020;30:R246–8.
26 Xie T, Fu D-J, Li Z-M, *et al*. Circsmarcc1 facilitates tumor progression by disrupting the Crosstalk between prostate cancer cells and tumor-associated Macrophages via miR-1322/Ccl20/Ccr6 signaling. *Mol Cancer* 2022;21:173.
27 Wang Y, Liu J, Ma J, *et al*. Exosomal circRNAs: Biogenesis, effect and application in human diseases. *Mol Cancer* 2019;18:116.
28 Yang C, Dou R, Wei C, *et al*. Tumor-derived Exosomal microRNA-106B-5P activates EMT-cancer cell and M2-subtype TAM interaction to facilitate CRC metastasis. *Mol Ther* 2021;29:2088–107.
29 Wang F, Li B, Wei Y, *et al*. Tumor-derived Exosomes induce Pd1+ macrophage population in human gastric cancer that promotes disease progression. *Oncogenesis* 2018;7:41.
30 Zhou Q, Xian M, Xiang S, *et al*. All-Trans retinoic acid prevents Osteosarcoma metastasis by inhibiting M2 polarization of tumor-associated Macrophages. *Cancer Immunol Res* 2017;5:547–59.
31 Wang H, Zhang J, Tian J, *et al*. Using dual-Tracer PET to predict the biologic behavior of human colorectal cancer. *J Nucl Med* 2009;50:1857–64.
32 Minard ME, Herynk MH, Collard JG, *et al*. The Guanine nucleotide exchange factor Tiam1 increases colon carcinoma growth at metastatic sites in an orthotopic nude mouse model. *Oncogene* 2005;24:2568–73.
33 Duranton B, Holl V, Schneider Y, *et al*. Polyamine metabolism in primary human colon adenocarcinoma cells (Sw480) and their lymph node metastatic derivatives (Sw620). *Amino Acids* 2003;24:63–72.
34 Qian M, Wang S, Guo X, *et al*. Hypoxic glioma-derived Exosomes deliver microRNA-1246 to induce M2 macrophage polarization by targeting Terf2Ip via the Stat3 and NF-KB pathways. *Oncogene* 2020;39:428–42.
35 Fu X-L, Duan W, Su C-Y, *et al*. Interleukin 6 induces M2 macrophage differentiation by Stat3 activation that correlates with gastric cancer progression. *Cancer Immunol Immunother* 2017;66:1597–608.
36 Liu Q, Yang C, Wang S, *et al*. Wnt5A-induced M2 polarization of tumor-associated Macrophages via IL-10 promotes colorectal cancer progression. *Cell Commun Signal* 2020;18:51.
37 Zhang Y, Zhang Z. The history and advances in cancer Immunotherapy: understanding the characteristics of tumor-infiltrating immune cells and their therapeutic implications. *Cell Mol Immunol* 2020;17:807–21.
38 Komai T, Inoue M, Okamura T, *et al*. Transforming growth factor-B and Interleukin-10 synergistically regulate humoral immunity via Modulating metabolic signals. *Front Immunol* 2018;9:1364.
39 Larionova I, Tuguzbaeva G, Ponomaryova A, *et al*. Tumor-associated Macrophages in human breast, colorectal, lung, ovarian and prostate cancers. *Front Oncol* 2020;10:566511.
40 Sarode P, Schaefer MB, Grimminger F, *et al*. Macrophage and tumor cell cross-talk is fundamental for lung tumor progression: we need to talk. *Front Oncol* 2020;10:324.
41 Wu J-Y, Huang T-W, Hsieh Y-T, *et al*. Cancer-derived Succinate promotes macrophage polarization and cancer metastasis via Succinate receptor. *Mol Cell* 2020;77:213–27.
42 Zhou X, Zhan L, Huang K, *et al*. The functions and clinical significance of circRNAs in hematological malignancies. *J Hematol Oncol* 2020;13:138.
43 Ashiru O, Boutet P, Fernández-Messina L, *et al*. Natural killer cell cytotoxicity is suppressed by exposure to the human Nkg2D ligand MICA*008 that is shed by tumor cells in Exosomes. *Cancer Res* 2010;70:481–9.
44 Wang S, Xu M, Li X, *et al*. Exosomes released by Hepatocarcinoma cells endow Adipocytes with tumor-promoting properties. *J Hematol Oncol* 2018;11:82.
45 Morrissey SM, Zhang F, Ding C, *et al*. Tumor-derived Exosomes drive immunosuppressive Macrophages in a pre-metastatic niche through Glycolytic dominant metabolic Reprogramming. *Cell Metab* 2021;33:2040–58.
46 Zhao S, Mi Y, Guan B, *et al*. Tumor-derived Exosomal miR-934 induces macrophage M2 polarization to promote liver metastasis of colorectal cancer. *J Hematol Oncol* 2020;13:156.
47 Xun J, Du L, Gao R, *et al*. Cancer-derived Exosomal miR-138-5p modulates polarization of tumor-associated Macrophages through inhibition of Kdm6B. *Theranostics* 2021;11:6847–59.
48 Xin L, Wu Y, Liu C, *et al*. Exosome-mediated transfer of lncRNA Hcg18 promotes M2 macrophage polarization in gastric cancer. *Mol Immunol* 2021;140:196–205.
49 Shang A, Gu C, Wang W, *et al*. Exosomal circPACRGL promotes progression of colorectal cancer via the miR-142-3p/miR-506-3P-TGF-B1 axis. *Mol Cancer* 2020;19:117.